AD-A067 710 MASSACHUSETTS INST OF TECH CAMBRIDGE AEROPHYSICS LAB F/G 4/1
SOME EFFECTS OF VEHICLE FLOW FIELD ON THE CAPTURE EFFICIENCY OF--ETC(U)
DEC 78 C W HALDEMAN, R H BUSH, S W PREY F19628-76-C-0185
UNCLASSIFIED MIT-TR-204 AFGL-TR-79-0009 NL

1 OF 1
ADA
067710

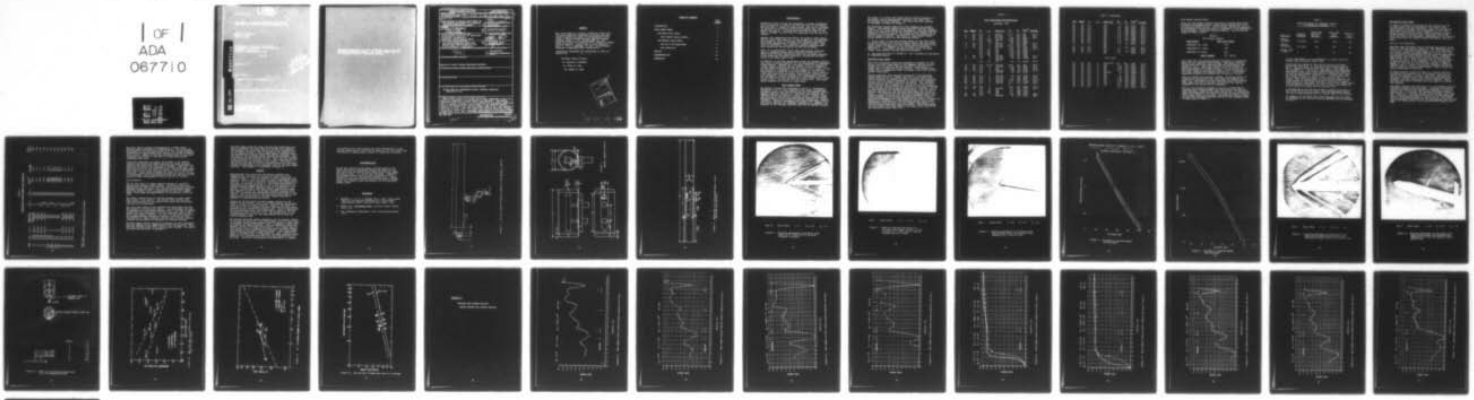

END
DATE
FILMED
6-79
DDC

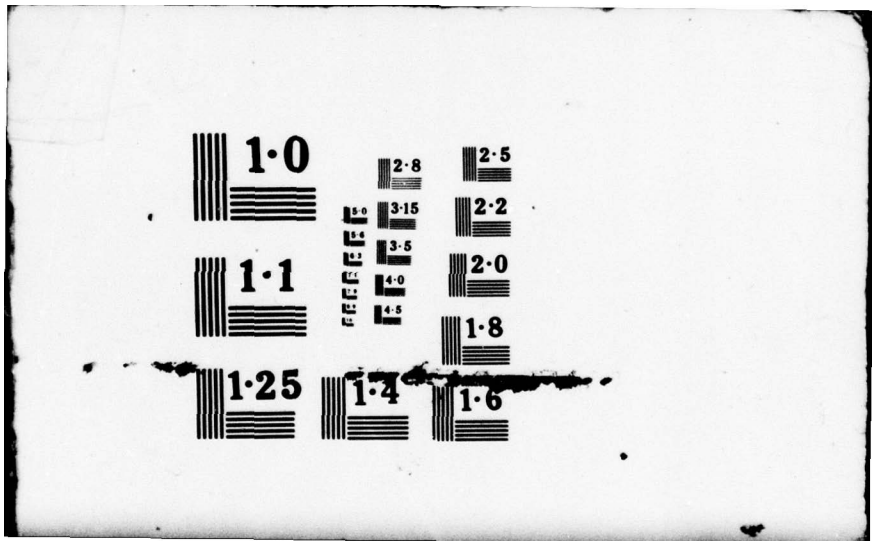
1·0
1·1
1·25
1·4
1·6
1·8
2·0
2·2
2·5
2·8
3·15
3·5
4·0
4·5

SECURITY CLASSIFICATION OF THIS PAGE (When Data Entered)

REPORT DOCUMENTATION PAGE

READ INSTRUCTIONS BEFORE COMPLETING FORM

1. REPORT NUMBER (19) (18) AFGL-TR-79-0009 (9) Final rept. 1 Oct 77-30 Sep 78
2. GOVT ACCESSION NO.
3. RECIPIENT'S CATALOG NUMBER

4. TITLE (and Subtitle) (6)
SOME EFFECTS OF VEHICLE FLOW FIELD ON THE CAPTURE EFFICIENCY OF A GERDIEN CAPACITOR ATMOSPHERIC PROBE

5. TYPE OF REPORT & PERIOD COVERED
Final
10/1/77 - 9/30/78

6. PERFORMING ORG. REPORT NUMBER (14)
MIT-TR-204

7. AUTHOR(s) (10)
Charles W. Haldeman,
Robert H. Bush
Scott W. Prey

8. CONTRACT OR GRANT NUMBER(s) (15)
F19628-76-C-0185

9. PERFORMING ORGANIZATION NAME AND ADDRESS
Massachusetts Institute of Technology
Aerophysics Laboratory
Cambridge, Massachusetts 02139

10. PROGRAM ELEMENT, PROJECT, TASK AREA & WORK UNIT NUMBERS
61102F
(16) 8605 1101 (17) 11

11. CONTROLLING OFFICE NAME AND ADDRESS (11)
Air Force Geophysics Laboratory
Hanscom AFB, Massachusetts 01731
Monitor/Edmund A. Murphy/LKD

12. REPORT DATE
December 1978

13. NUMBER OF PAGES
40

14. MONITORING AGENCY NAME & ADDRESS (if different from Controlling Office)
(12) 41 p.

15. SECURITY CLASS. (of this report)
Unclassified

15a. DECLASSIFICATION/DOWNGRADING SCHEDULE

16. DISTRIBUTION STATEMENT (of this Report)

Approved for public release; distribution unlimited.

17. DISTRIBUTION STATEMENT (of the abstract entered in Block 20, if different from Report)

18. SUPPLEMENTARY NOTES

19. KEY WORDS (Continue on reverse side if necessary and identify by block number)

Ground testing, atmospheric probe, Gerdien capacitor, supersonic flow

20. ABSTRACT (Continue on reverse side if necessary and identify by block number)

Wind tunnel tests of a rocket borne upper atmospheric probe for measuring atmospheric charge density are reported. The Gerdien capacitor probe consists of a short section of a co-axial capacitor. This is mounted on pylons from a model of the Tomahawk vehicle. Results are reported for the mach number range 2 to 3 and altitude range 26 to 50 km. Over this range the ratio of mass flow through the probe to mass flow in an equal cross section of the free stream ranged from .69 to .80. Schlieren photographs of the flow are presented.

DD FORM 1 JAN 73 1473

Unclassified

SECURITY CLASSIFICATION OF THIS PAGE (When Data Entered)

009200

79 04 19 031

PREFACE

This Final Report on Contract F19628-76-C-0185 with Air Force Geophysics Laboratory describes work performed studying the effect of the aerodynamic flow field on vehicle-mounted Gerdien capacitor probes between October 1, 1977 and September 30, 1978, under the technical cognizance of Mr. Edmund A. Murphy, Contract Monitor. Earlier work on this contract, April 1, 1976 to September 30, 1977, was previously reported in AFGL TR-77-0210 (Reference 1).

Professional personnel who contributed to this research are:

Professor Morton Finston

Dr. Charles W. Haldeman

Mr. Scott W. Prey

Mr. Robert H. Bush

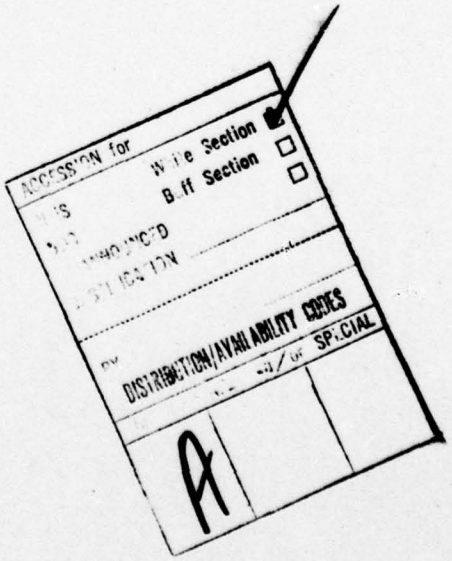

TABLE OF CONTENTS

	Page Number
INTRODUCTION	3
WIND TUNNEL TESTS	3
One-Tenth Scale Tests	4
Wind Tunnel Sealing Effort	7
One-Quarter Scale Tests	9
Set-up of the Experiment	9
Data Reduction	11
RESULTS	12
RECOMMENDATIONS	13
REFERENCES	13

INTRODUCTION

Supersonic flight through the atmosphere is always accompanied by the formation of a shock wave near the nose of the vehicle. When the body is slender and sharp nosed, this wave is attached to the point at an oblique angle and propagates away from and behind the vehicle. In cases where the body is blunt or the nose is rounded, the shock wave is displaced from the nose (detached).

Because both temperature and density are several times higher behind a shock than ahead of it, the presence of the shock must be included in order to determine free atmosphere properties from those measured near a supersonic sounding rocket. Thus tests to calibrate a flow sensitive property sampling probe must involve the entire vehicle as well as the probe.

Tests of a nose-mounted conical mass spectrometer probe for use on a Tomahawk vehicle were previously carried out (1). These tests provided information about the up-stream influence of the probe and furnished calibration corrections for data taken at altitudes above 70 Km.

In addition to the mass spectrometer probe the Tomahawk vehicle will carry a Gerdien capacitor for the measurement of atmospheric charge density. Because this instrument cannot be deployed at a great enough distance from the vehicle to place it ahead of the bow shock as determined from the recent M.I.T. tests, it will be necessary to calibrate it in the presence of the vehicle. Under Contract F19628-76-C-0185 P0005-0008 wind tunnel tests of a one-tenth scale and one-quarter scale Gerdien capacitor have been conducted. Results indicate that disgorgement altitude for the shock wave from the Gerdien is above 58 Km at M=3, about 49 Km at M=2.5; 41 Km at M= 2.25 and 35 Km at M=2. This Final Report presents the results of these tests.

WIND TUNNEL TESTS

Two series of tests were conducted in the M.I.T. Aerophysics Laboratory's 18 x 24 inch supersonic wind tunnel to determine the shock pattern and flow calibration for the Tomahawk vehicle Gerdien capacitor combination. The model configuration and capacitor detail are shown in Figures 1 and 2. Figure 3 shows the cavities in the body for mounting the capacitor and probe. Capacitor details were scaled from Adcole Corporation, drawing D-12982-A. Mounting arrangement and support were taken from an AFGL layout drawing (not numbered) supplied by E. McKenna. Deployment of the Gerdiens required that they be mounted slightly

off center (1.5 inches full scale) and be located outboard of a rectangular cavity approximately one-half inch larger than the Gerdien envelope dimension. The cavity was also included in the model, as shown in Figure 3.

One difference between model and flight geometry was present, however. The Gerdien support pylons were made oversize (twice scale size) and round instead of rectangular. This was necessary because of the small size of the one-tenth scale Gerdien and was preserved on the one-quarter scale model for consistency and to provide needed stiffness. The effect of these larger support pylons should be small for the following reasons:

1. While larger in size the blocking effect of the twice scale cylindrical pylons will be only slightly larger than full-scale square pylons because of the much larger drag coefficient of the square pylon (1.7 compared to .94 for bodies of revolution, Reference 2. Long pylons, because they are nearly two dimensional, would exhibit on even greater difference).

2. The capacitor inlet is forward of the influence of the pylons at supersonic speeds.

<u>One-Tenth Scale Tests</u>

The first preliminary tests were conducted in December of 1977 using a one-tenth scale model of the Tomahawk vehicle with 35° skimmer nose and Gerdien capacitor mounted at positions 5.5 inches and 6.2 inches aft of the nose tip. Other details were scaled from the dimensions shown in Figures 1 and 2 for the one-quarter scale model.

Because experience had indicated resolution of the Schlieren system would be poor on a model this size at the lowest wind tunnel pressures, an attempt was made to produce flow visualization by using the Gerdien capacitor to create a glow discharge between the two Gerdien electrodes and ground. This produced a glow discharge when connected to a 10,000 volt 10-100 ma power supply but the visible region was confined to the area downstream of the Gerdien and shock position could not be inferred. Use of the glow discharge was therefore discontinued. Data for the remaining conditions for the one-tenth scale model are listed in Table 1. As observed from the Schlieren photographs and on the viewing screen, the shock wave was always attached at M=3, was always detached at M=2 and was detached above 28 Km at M=2.5. Schlieren photographs for three conditions are shown in Figures 4-6. Because of a malfunction in the Schlieren system, much of the photographic data for Runs 1-22 was unusable (see Figure 5) to confirm visual observation during the tests. Extensive repairs were made before the later tests at one-tenth scale, Runs 23-34 and one-quarter scale, Runs 1-20.

Table 1

1/10 Scale Model Run Conditions

December, 1977

Run	Model	M	α	Photo No.	P_o	T_o	$Re_D 10^6$	Alt(Km)
1	62	3.0	0	65143-4	15.0	110	.222	32.1
2	62	3.0	0	145-146	7.1	105	.105	34.2
3	62	3.0	0	147-148	3.04	115	.0450	40.9
	62	3.0	0-10	149-150	3.05	120	.0451	
		3.0	+10	151	3.08	122	.0456	
4	62	3.0	0	152-153	.60	112	.0089	51.5
5	55	3.0	0	656-157	15.0	114	.222	32.1
6	55	3.0	0	058-159	6.97	135	.1031	35.0
		3.0	0	160	7.07	95	.1046	34.4
		3.0	-10	161	7.06	100	.1045	
		3.0	+10	162	7.08	102	.1048	
		3.0	+20	163	7.05	106	.1043	
7	55	3.0	0	164-165	2.96	112	.0438	41.1
8	55	3.0	0	166-167	.58	102	.00858	51.8
				168-169				
		3.0	10	174	.55	98	.00814	52.2
9	55	2.0	-9,+10	178-182	15.0	104	.363	26.6
10	55	2.0	0	183-184	6.88	113	.1665	31.1
11	55	2.0	0	185	2.98	98	.0721	35.8
12	55	2.0	0	186-187	.60	100	.0145	45.4
		2.0	0	188-189	.59	100	.0143	
13	62	2.0	0	190-190	.58	108	.0140	45.6
13	62	2.0	0	192-193	.6	100	.0145	45.4
14	62	2.0	0	194-195	2.98	108	.0721	35.8
15	62	2.0	0	196-197	7.1	115	.1718	30.9
16	62	2.0	0	198-199	15.1	110	.3654	26.7
17	62	2.5	0		15.1	107	.2884	29.5
18	62	2.5	0	203-204	7.0	110	.1337	34.0
		2.5	-8	205	7.0	108	.1337	
		2.5	+10	206	7.0	108	.1337	
19	62	2.5	0	207	3.0	108	.0573	38.5
20	62	2.5		208-209	.60	103	.0115	48.3

Table 1 (continued)

Run	Model	M	α	Photo No.	P_o	T_o	$Re_D 10^6$	Alt(Km)
21	62	2.5		210	.9	104	.0172	45.7
21	62	2.5		211	1.0	104	.0191	44.9
21	62	2.5		212	1.1	105	.0210	44.5
21	62	2.5		213	1.2	105	.0229	44.0
21	62	2.5		214	1.3	106	.0248	43.3
21	62	2.5		215	1.5	107	.0287	42.4
21	62	2.5		216	1.4	107	.0267	42.8
21	62	2.5		217	1.3	107	.0248	43.3
21	62	2.5		218	1.2	107	.0229	44.0
21	62	2.5		219	1.1		.0210	44.5
21	62	2.5		220	1.0	109	.0191	44.9
				221				
22	62	2.5		222	3	101	.0573	38.5
22	62	2.5		223	1.5		.0287	42.5
22	62	2.5		224	1.4	102	.0267	43.0
22	62	2.5		225	1.3		.0248	43.2
				July, 1978				
23	62	2.5	0	65497-500	10.1	88.5	.1929	31.6
23	62	2.5	0	501	5.0	108	.0955	35.6
23	62	2.5	0	502	2.94	107	.0562	38.5
24	62	2.5	0	503	2.04	108	.0390	40.7
25	62	2.5	0	504	1.0	107	.0191	45.0
26	62	2.5	0	505-506	.47	103	.00898	50.1
27	62	2.5	0	507	.6	103	.0115	48.5
28	62	2.5	0	508	.8	104	.0153	46.5
29	62	2.5	0	509	1.04	106	.0199	44.9
30	62	2.5	0	510	1.20	106	.0229	43.5
31	62	2.5	0	511	1.50	108	.0287	42.4
32	62	2.5	0	512	2.0	110	.0382	40.7
33	62	2.5	0	513	3.0	110	.0573	38.4
34	62	2.5	0		4.0	110	.0764	36.9

Wind Tunnel Sealing Effort

Since the wind tunnel pressure could not be lowered sufficiently to produce detachment at M=3, a minor effort was devoted to improving wind tunnel sealing. First existing leakage was measured by successively sealing the shafts on Compressor 1 and Compressor 2 using "Duxseal", a moldable claylike material. The results are listed in Table 2 below.

Table 2

Wind Tunnel Leakage

Leak Source	Mass Flow lb/sec
Compressor #1, seals	.125
Compressor #2, seals	.055
Remainder of tunnel	.07
Total Leakage	.25 lb/sec

This shows that the minimum pressure obtainable is controlled mainly by the compressor seal leakage. Additional external Teflon sheet seals were therefore made and installed on Compressors 1 and 2. Each seal consisted of three washers of one-thirty-second thick Teflon sheet, split to go over the shaft and formed to a curved lip shape. Static evacuation of the tunnel produced the expected results; i.e., the minimum stagnation pressure was reduced from .48 psia to .14 psia.

After ten minutes of operation, however, the Teflon wore, increasing the clearance to the point where the pressure was again .48. This result was not surprising since the original inner labyrinth seal was holding .48 psia and the running clearance on the seals must be comparable.

While it was originally planned to set up a vacuum pump to intercept seal leakage between the outer Teflon seal and the inner labyrinth, time did not permit doing this. If additional tests are conducted in the future, this can be done now that the Teflon outer seals are in place. The predicted effect of pumping with the available Beach-Russ RP-750 on the interseal space is shown below in Table 3.

Table 3

Predicted Effect of Interseal Pumping on Stagnation Pressure

Condition	Interseal Pressure	Pumped Seal Leak Rate lbs/sec	Total Seal Leak lbs/sec	Tunnel P_o (psi)
Pumping #1 seals	1.9 psia	.016	.141	.28
Pumping #1 and #2	2.7 psia	.033	.08	.16
Perfect seal 1 and 2	0	0	.07	.14

If this improvement can be implemented, it should raise the highest test altitude by about 8 Km.

During the last series of runs (23-34) with the one-tenth scale model (see Table 1), Schlieren pictures were taken at M=2.5. Figure 4 shows the flow about the .1 scale model at 31.6 Km and M=2.5. The shock is swallowed in this photograph. These repeat runs at M=2.5 were made to observe the effect of altitude on disgorgement since the early Schlieren data could not be used because of a malfunction. A typical photo from this series is shown in Figure 5 at M=3 and 32.1 Km. In Figure 4 note the large number of disturbances created by the various parts of the Gerdien structure, including the shear layer behind the lower edge. The shear layer at the upper edge is inclined downward because of the flow of shock decelerated air in from behind the pylons into the Gerdien wake.

A detached shock position can be seen in Figure 6 for Run 9 at M=2, $\alpha=10^{o}$ and 26.6 Km altitude. Here the detachment bubble can just be seen emerging from the inboard edge of the Gerdien.

In summary, the one-tenth scale data indicated that the shock was attached at M=3 and M=2.5 and was detached for all altitudes at M=2.0.

One-Quarter Scale Tests

In order to determine quantitatively what fraction of the on-coming mass flow was swallowed by the Gerdien under various shock attachment conditions, tests of a one-quarter scale model were carried out in September of 1978. This model was large enough to permit impact pressure surveys to be made behind the Gerdien with a traversing impact tube. Since the Gerdien was detachable, measurements of the velocity distribution near the vehicle without the Gerdien were also made.

Set-up of the Experiment

The tests were performed using an aluminum one-quarter scale model of probe and Gerdien capacitor. The experiment was run in the M.I.T. Aerophysics Laboratory's 18" x 24" supersonic wind tunnel operating at Mach numbers of 2.25 and 2.0. The run conditions were determined from test section temperatures and pressure data read from the control panel. Stagnation temperatures varied near 110^{o}F and total pressures ranged from .6 to 5 psia. These conditions gave an altitude range of approximately 25 to 45 kilometers. A plot of Reynolds number vs. altitude for the full-scale vehicle is shown in Figures 7 and 8. Figure 7 was used to determine equivalent test altitude from test Reynolds number. Table 4 lists the tunnel conditions for each run.

An impact pressure survey was taken at a station one-half inch behind the centerline of the condenser, both with and without the condenser in place. This data, combined with the static pressure, gave a Mach number profile behind the condenser, and also the profile with no condenser. These profiles were used to determine the total mass flow through the condenser.

The impact pressure was read using a 2.5 psia Statham pressure transducer mounted inside the model. The probe was mounted with the tip one-half inch behind the condenser on a pair of support rods. One support was threaded and passed through a gear driven nut. The other passed freely through a ball bushing. Position was measured by reading the voltage developed across a potentiometer geared to the nut drive. The output from the pressure transducer and the potentiometer were plotted using a HP 7044A plotter, the end points being checked with a DVM.

Table 4

One-Quarter Scale Model Run Condition

Run	M	α	Photo No.	P_o	T_o	$Re_D 10^6$	Alt(Km)	$\frac{\dot{m}}{\dot{m}_{f.s.}}$
1	2.25	0	65526-528	5	110	.269	29.6	.801
2	2.25	-10-+15	529-534	5	110			
3	2.25	0	538	3	110	.161	32.9	.784
4	2.25	-10-+15	539-544	3	103			
5	2.25	0	545	1.5	105	.0806	37.5	.752
6	2.25	-10-+15	546-558	1.5	105			
7	2.25	0	559	.63	108	.0339	43.8	.739
8	2.25	-10-+15	560-573	.63	100			
* 9	2.25	0	574	1.5	100	.0806	37.5	.793
* 9a	2.25	0	575	1.5	102	.0806	37.5	
*10	2.25	0	576	.64	102	.0344	43.7	.813
*10a	2.25	0	577	.64	110	.0344	43.7	
*11	2.0	0	578	1.5	110	.0908	35.9	.839
*11a	2.0	0	579	1.5	106	.0908	35.9	
*12	2.0	0	560	.6	106	.0363	42.2	.809
*12a	2.0	0	581	.6	110	.0363	42.2	
13	2.0	0		5.0	110	.3025	28.9	.698
14	2.0	-13-+15	582-589	5.0	110			
15	2.0	0	590	3.0	110	.1815	31.4	.758
16	2.0	-10-+15	591-596	3.0	110			
17	2.0	0	597	1.5	110	.0908	35.9	.734
18	2.0	-10-+15	598-603	1.5	110			
19	2.0	0	604	.64	110	.0387	42.3	.689
20	2.0	-10-+15	605-619	.64	110			

*Runs with Gerdien removed and hole plugged.

The local static pressure was measured by a needle static pressure probe connected to the MKS Baratron. The probe read the pressure at an equivalent position to that of the condenser centerline and impact probe axial station but located 90 degrees out of plane. Because of the many standing waves and flow disturbances, see Figure 9, this use of a fixed static probe introduced some error.

During the experiment the tunnel was brought to the desired condition and stabilized before starting the impact pressure traverse and reading the local static pressure. Tests were run both with and without the condenser at various conditions. Traverses were made at zero angle of attack. Schlieren photographs were taken at zero angle of attack and from -10^{o} to $+15^{o}$ at 5^{o} intervals. These helped determine the effect of angle of attack on disgorgement, which was negligible below 10^{o} and small at 15^{o}. Figure 10 shows disgorgement at M=2.25 and 15^{o} at 43.8 Km.

Data Reduction

The raw data plots of impact pressure voltage vs. position voltage were reduced to Mach number. The probe position was determined from these plots with the initial and final positions measured during the tests. The position-potentiometer output slope was assumed linear and determined for each run independently. This slope was approximately .59 volts/inch in all the runs.

The impact pressure data was reduced assuming a linear transducer output (.124 psi/mV). The voltage read from the data plot were corrected for the plotter gain using the end voltage read during the experiment.

The local Mach number at the condenser was determined from the Mach angles in the Schlieren photos. This Mach number was used to determine the free stream pressure ratio. The static pressure reading was then corrected to give this pressure ratio at the end of the pressure traverse. In this test the static pressure was assumed constant through the profile, although the wide fluctuations in impact pressure indicate that a static pressure traverse of the profile is necessary for maximum accuracy.

The Mach number profile behind the condenser was then determined from the pressure ratio (impact/static) and the position. This data was reduced on the PDP-11 using a basic program. The resulting plots are presented in Appendix A.

The Mach number profiles along with the free stream data were used to determine the total mass flow through the condenser. The condenser was considered broken into strips perpendicular to the radial traverse. This is equivalent to assuming that the disturbances from the center-body support propagate across the width of the condenser before leaving the condenser. The integration was done assuming the flow field from the condenser to be elliptical at the probe station. This accounted for the expansion around the blockage by the support. The height of the ellipse was taken to be the distance between the low speed regions corresponding to the condenser walls in the Mach number profiles. This scheme is illustrated in Figure 11.

RESULTS

Measured mass flow ratios for the Gerdien condenser are summarized as a function of altitude in Figure 12 and are listed in Table 4. Here the results are more complicated than expected, with no clear cut effect of shock disgorgement being apparent. This is not surprising considering the complexity of the flow, as pictured in Figure 9. The complicated system of compressions and expansions set up by the nose produces a non-uniform and Mach number dependent flow in the absence of the Gerdien. Perturbations from both Gerdien supports and center body supports as well as the Gerdien cylinders interact with this flow to produce the complicated pattern downstream of the Gerdien. This gives rise to the very wavy pattern seen by the impact probe and displayed in the Mach number profiles in Appendix A, Figures A1-A4 and A7-A10.

Figures A5 and A6 present the Mach number profiles in the absence of the Gerdien. Here at both Mach numbers the boundary layer is thicker at higher altitude. However, the effect of altitude on the flow between the shock wave and the body alters conditions just outside the boundary layer. This is responsible for the different growth rates exhibited in Figure 13 for the thickness to reach .6 M_∞ and .9 M_∞. The dotted curve in this figure appears to best fit the experimental growth rate for vehicle boundary layer.

The effects mentioned appear responsible for the general scatter in the data on Figure 12. Here there seems to be no clear effect of attached versus disgorged shock with a tendency to lower mass flow ratios at higher altitudes. Here the measured values vary between .69 and .80 between 42 and 30 Km. It is likely some of this scatter could be reduced by taking static pressure surveys simultaneously with impact pressure surveys. This would remove some of the uncertainty in data reduction. Also, widening the range of available data to include M=3 and lower altitudes would point out if a constant mass flow ratio was approached at low altitude. Looking at the presently available data, it appears

that Gerdien flow ratio factors may vary from about 85 to 90% of free stream near M3 and 10 Km to nearer 60% at M=2.3 and 90 Km. Plotting to a log/log scale, Figure 14 shows this variation.

RECOMMENDATIONS

Future work should include higher altitude tests at the Arnold Engineering Development Center and additional surveys using the one-quarter scale model with both an impact and static probe. If a flight was available, a specially nose-mounted Gerdien could be used to provide a direct calibration for two side-mounted condenser units. Higher values of calibration factors could be obtained if Gerdien center body supports were constructed in a low drag aerodynamic shape.

REFERENCES

1. Haldeman, c. W., R. A. Kraemer and B. Ziph, "Wind Tunnel Tests of the Upstream Influence of a Conical Mass Spectrometer Probe", AFGL-TR-77-0210, Sept., 1977.

2. Hoerner, S., Aerodynamic Drag, Otterbein Press, Dayton, Ohio, 1951.

3. U.S. Atmosphere Supplements, 1966, Mid-Latitude Spring-Fall.

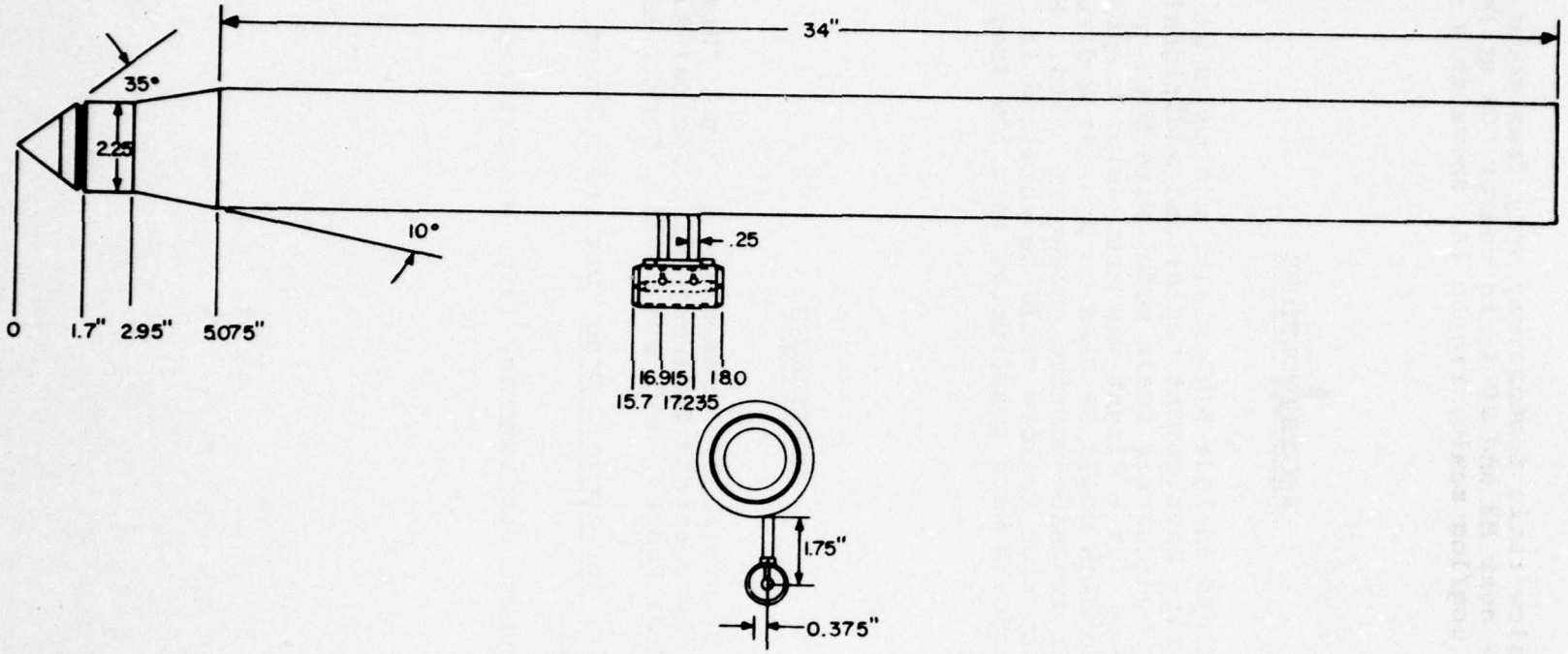

Figure 1. 1/4 scale model of Gerdien capacitor and Tomahawk vehicle.

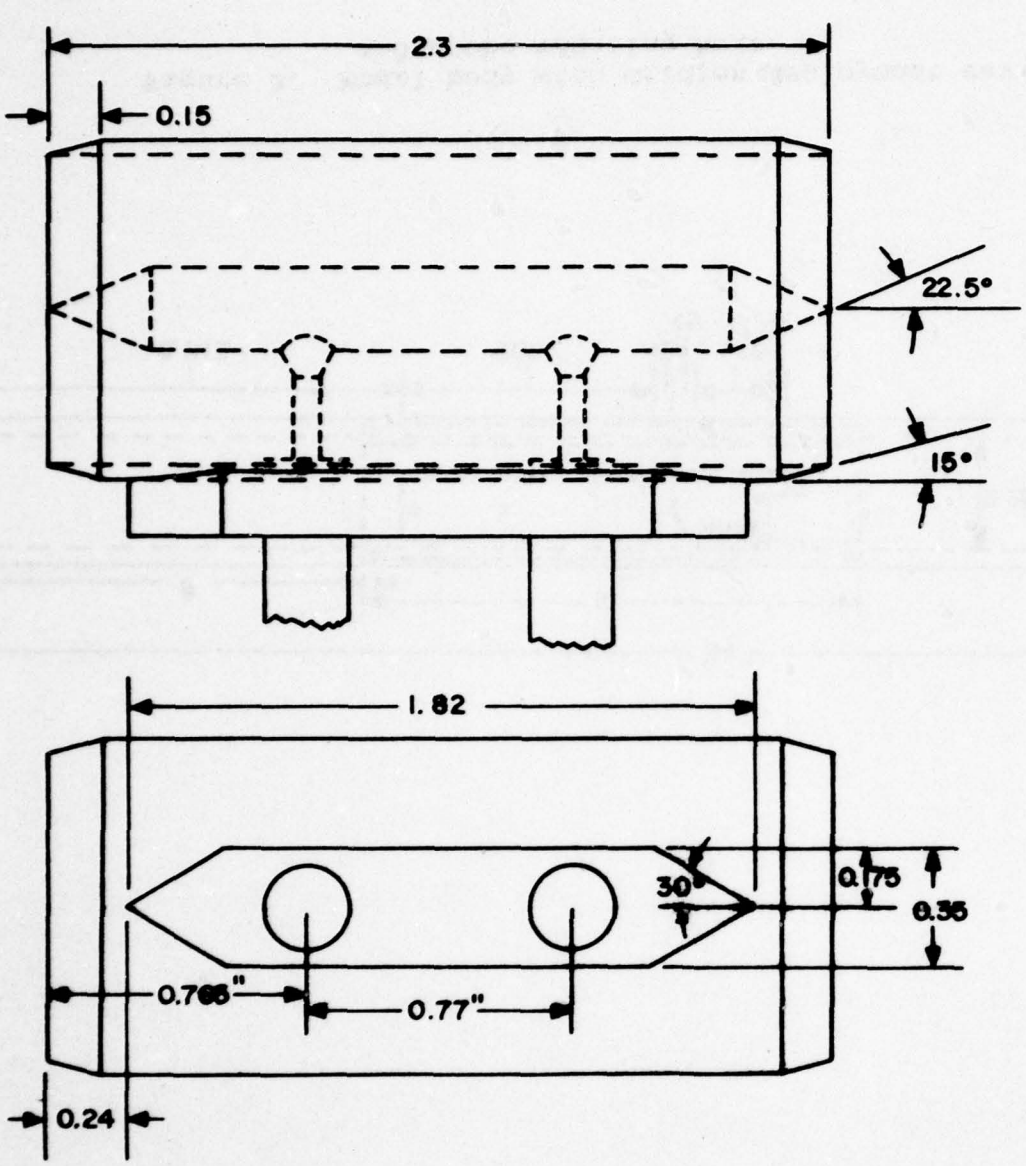

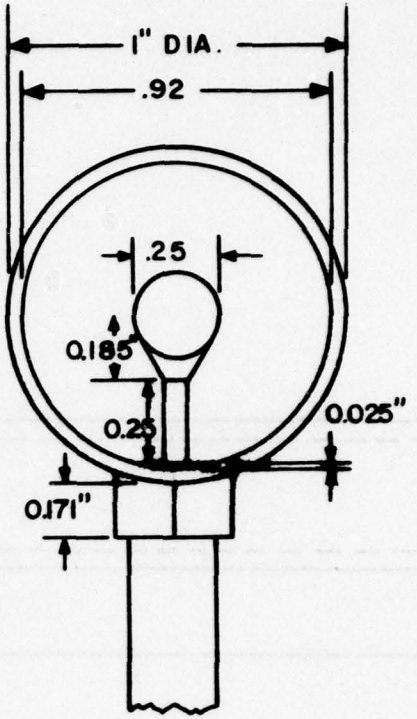

Figure 2.

Gerdien capacitor detail.

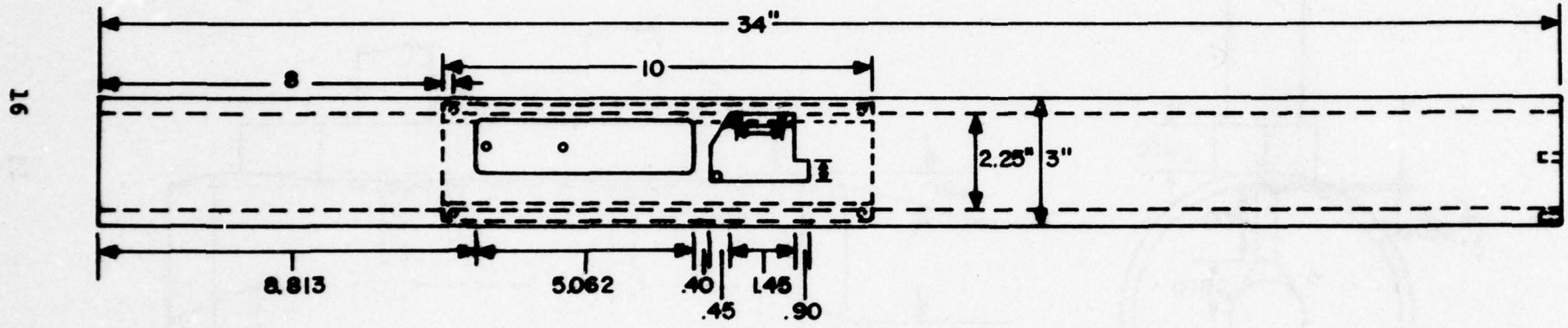

Figure 3. Model body with Gerdien deployment cavity and probe mounting hole.

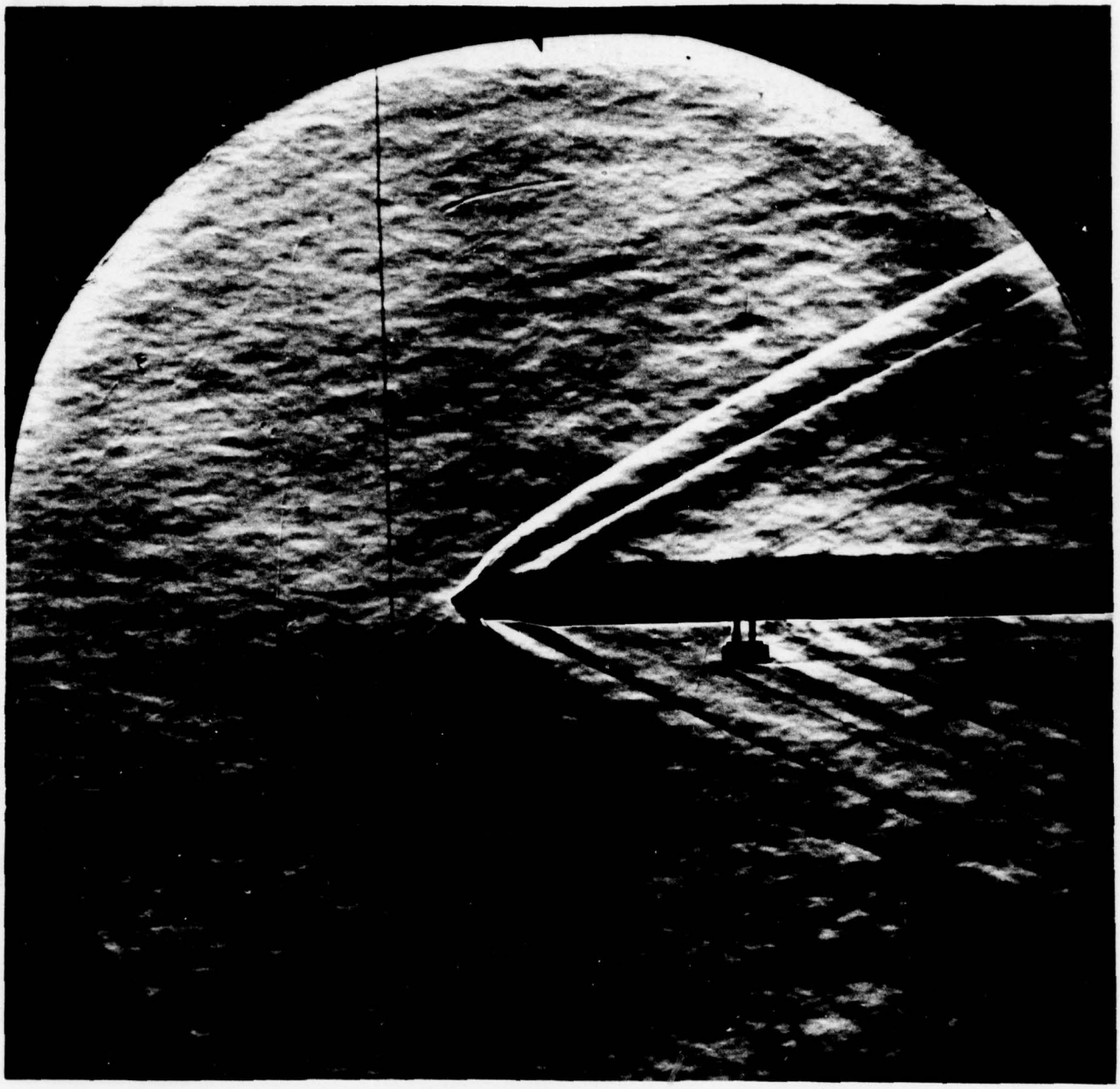

Run 23 Photo 65498 $\alpha = 0$ $M = 2.25$ $P_o = 10$

Figure 4. Schlieren photograph of one-tenth scale model at M = 2.25 and 31.6 Km shock attached to Gerdien.

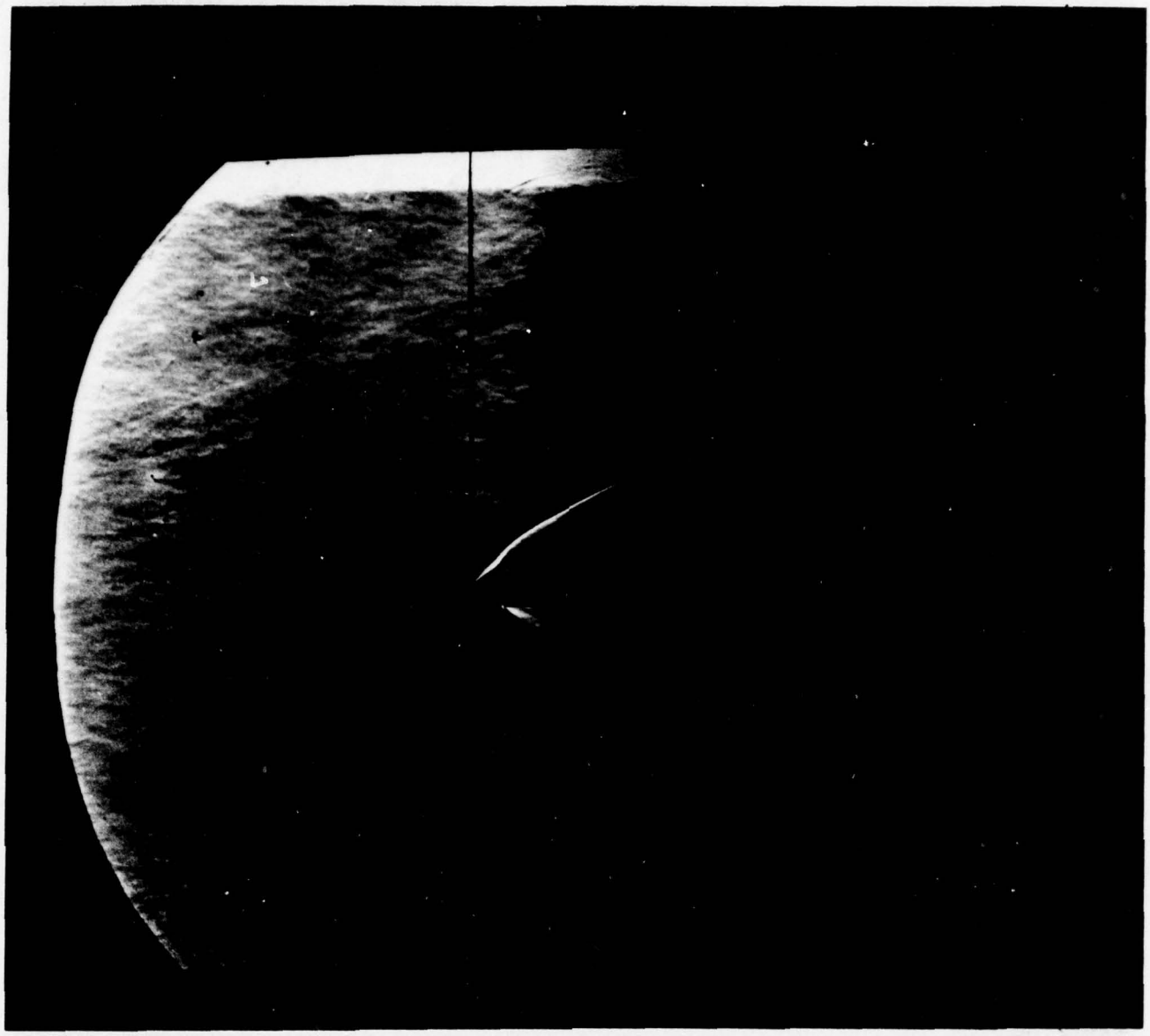

Run 1 Photo 65143 $\alpha = 0$ M = 3 $P_o = 15$

Figure 5. Defective Schlieren photograph of one-tenth scale model typical of much of Runs 1-22. Shock wave on Gerdien attached but not visible.

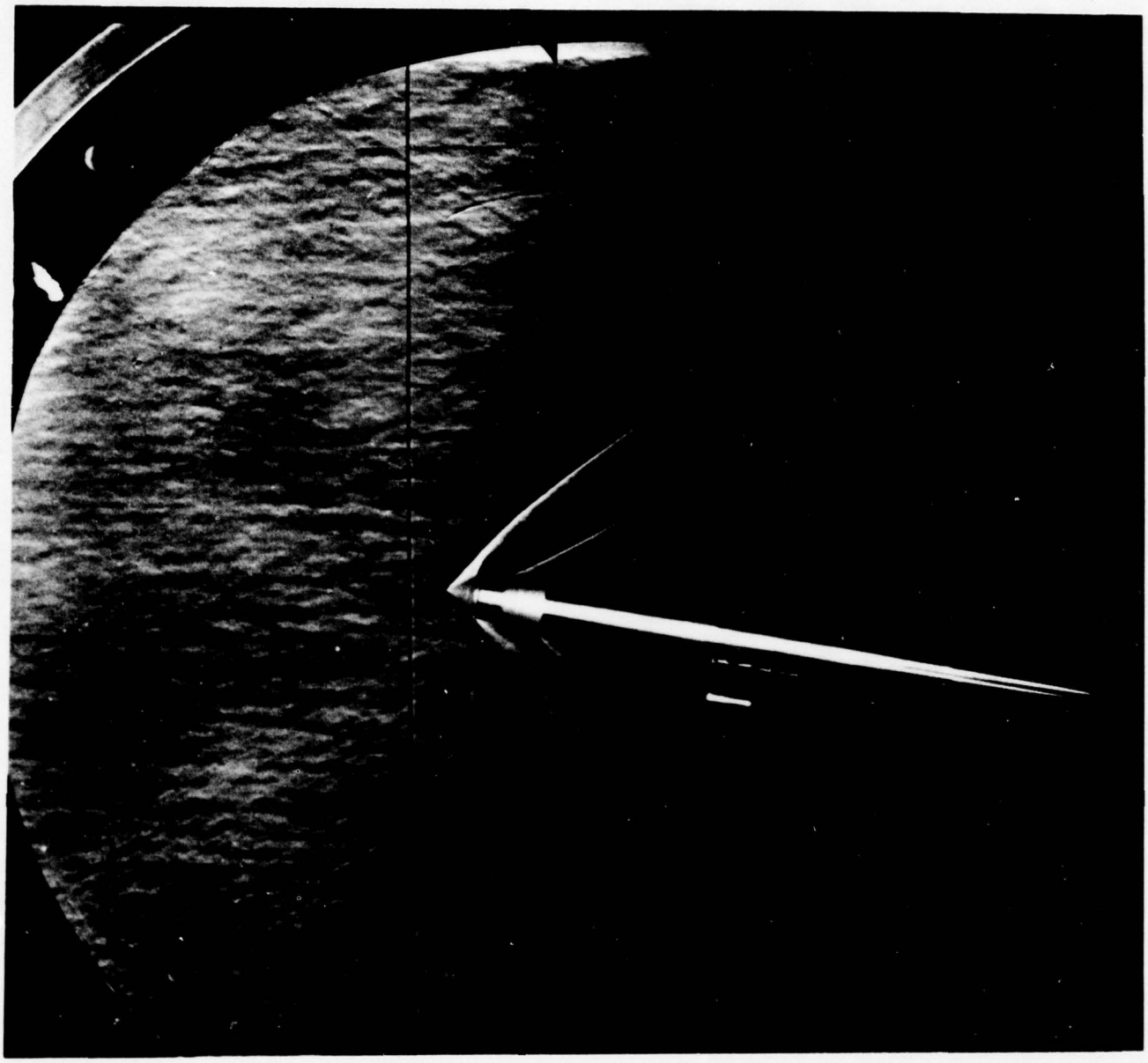

Run 9 Photo 65181 $\alpha = 10^{o}$ M = 2.0 $P_o = 15$

Figure 6. Schlieren photograph of one-tenth scale model showing shock wave detached from Gerdien at M = 2 and 26.6 Km.

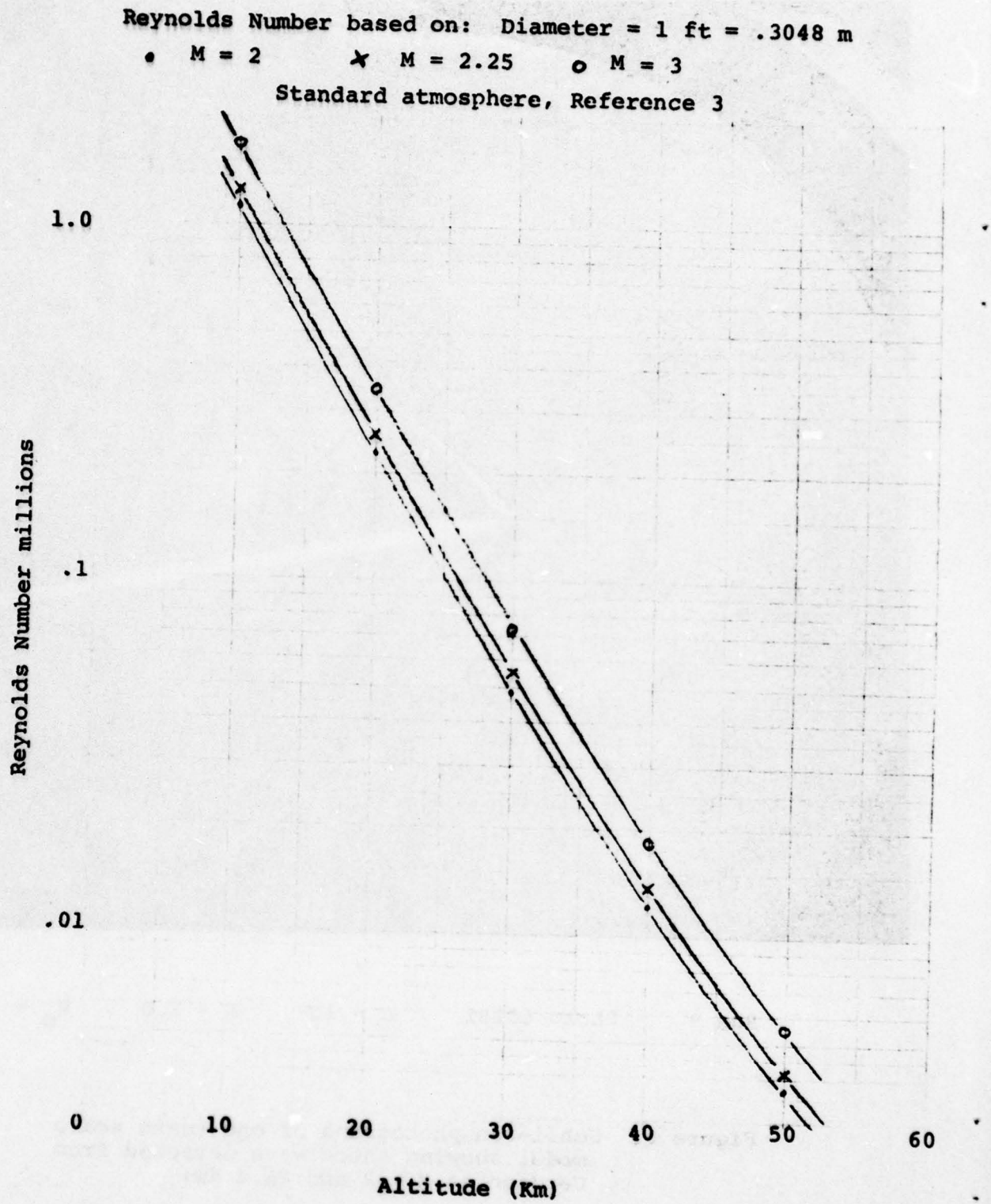

Figure 7. Altitude vs. Reynolds Number
Low Altitudes

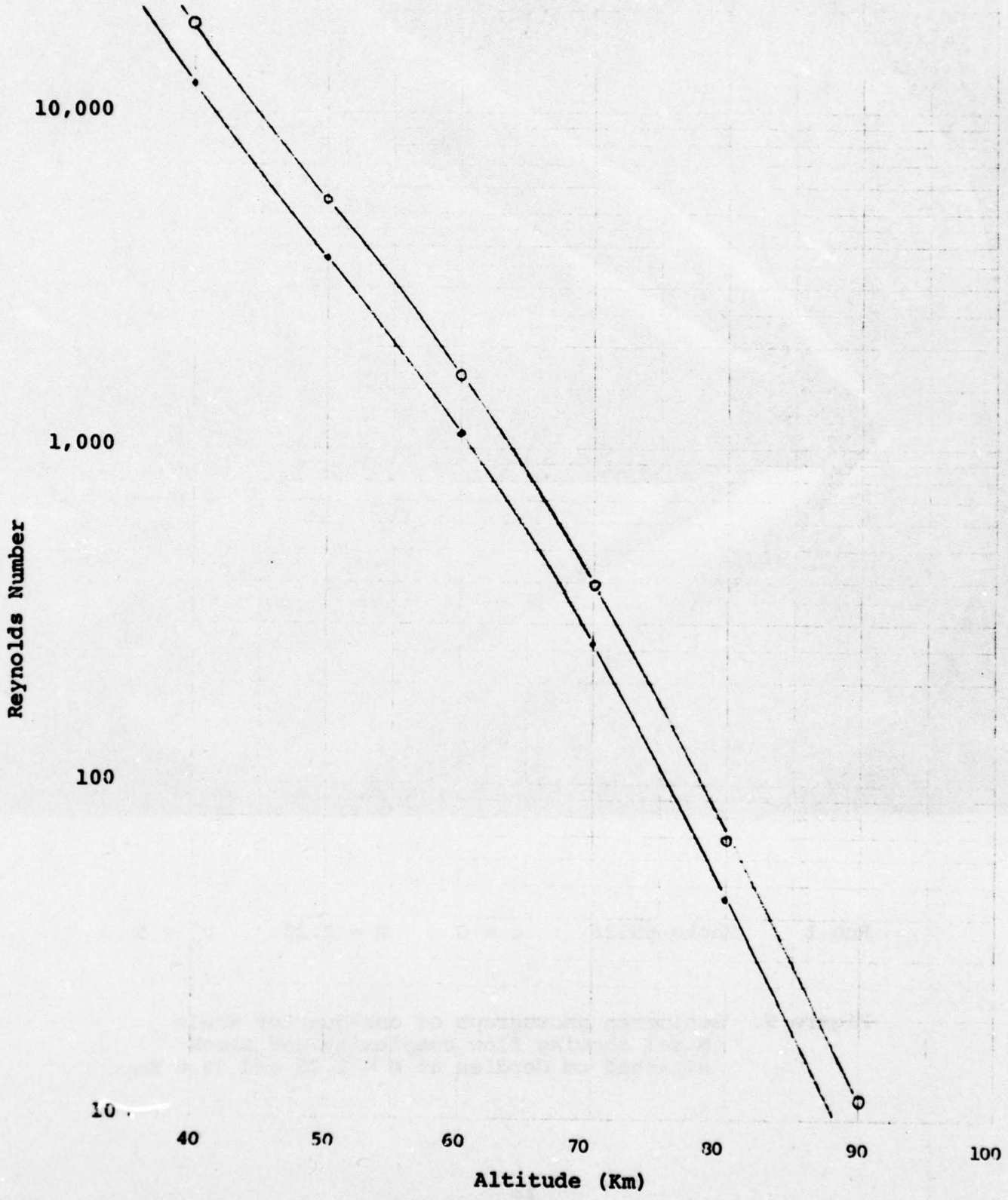

Figure 8. Altitude vs. Reynolds Number
High Altitudes

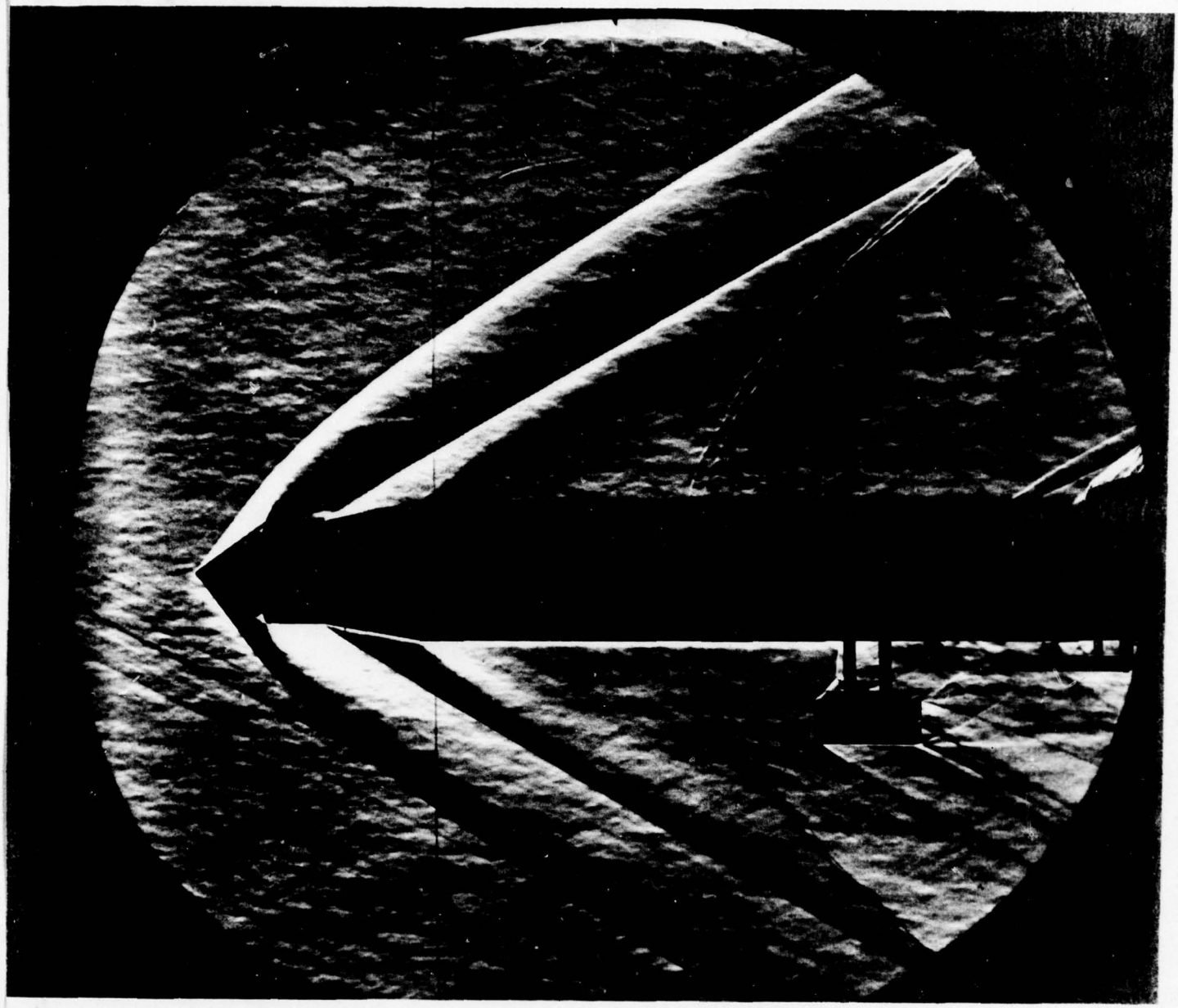

Run 1 Photo 65526 $\alpha = 0$ M = 2.25 $P_o = 5$

Figure 9. Schlieren photograph of one-quarter scale model showing flow complexity and shock attached to Gerdien at M = 2.25 and 26.6 Km.

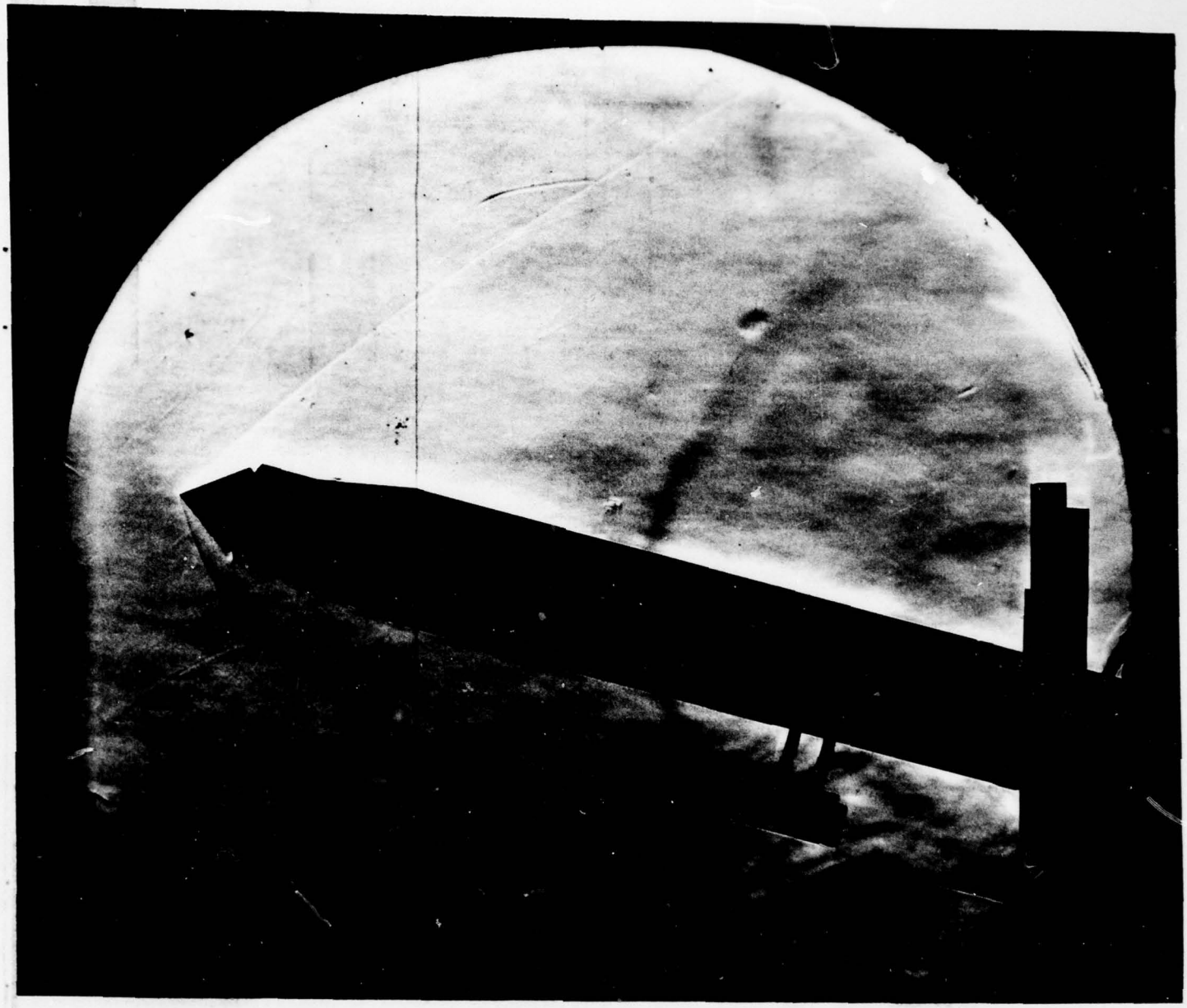

Run 8 Photo 65573 $\alpha = 15^{o}$ M = 2.25 $P_{o} = .63$

Figure 10. Schlieren photograph of one-quarter scale model showing shock wave detached from Gerdien at M = 2.25, 15^{o} angle of attack and 43.6 Km.

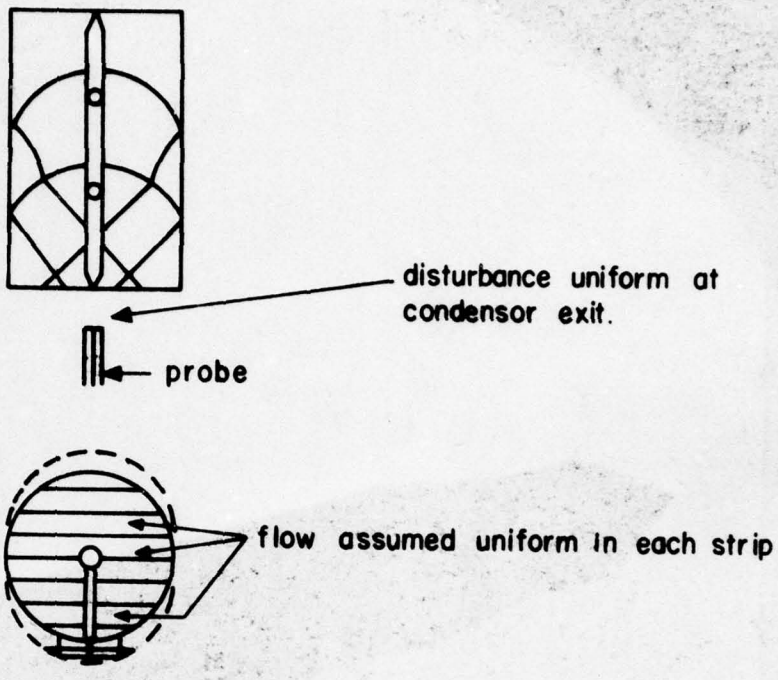

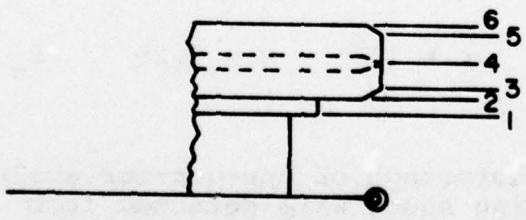

Station	X
1	1.15
2	1.32
3	1.37
4	1.82
5	2.27
6	2.32

Figure 11. Model for calculating average mass flow from measured profile.

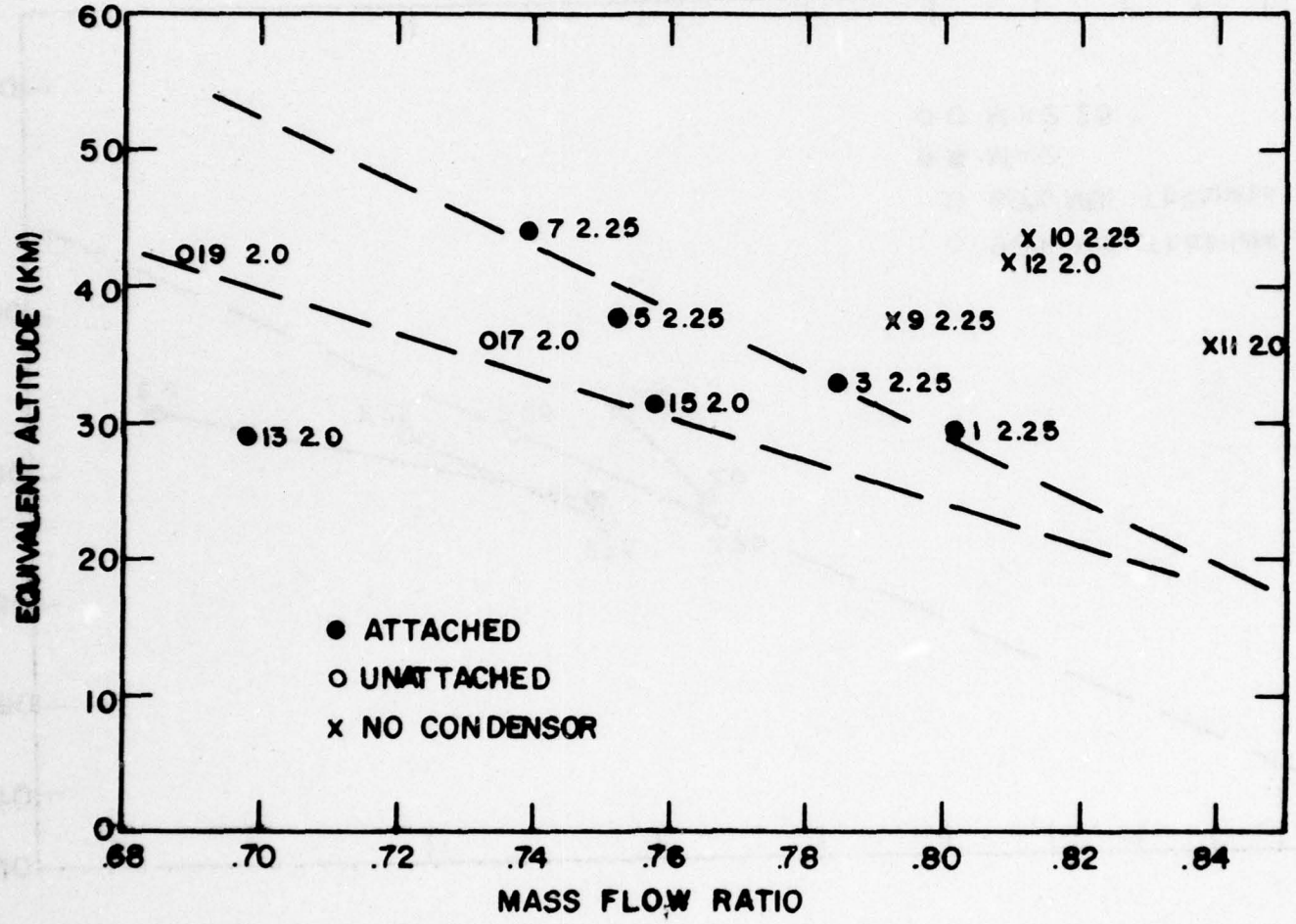

Figure 12. Mass flow ratio as a factor of altitude from 1/4 scale tests.

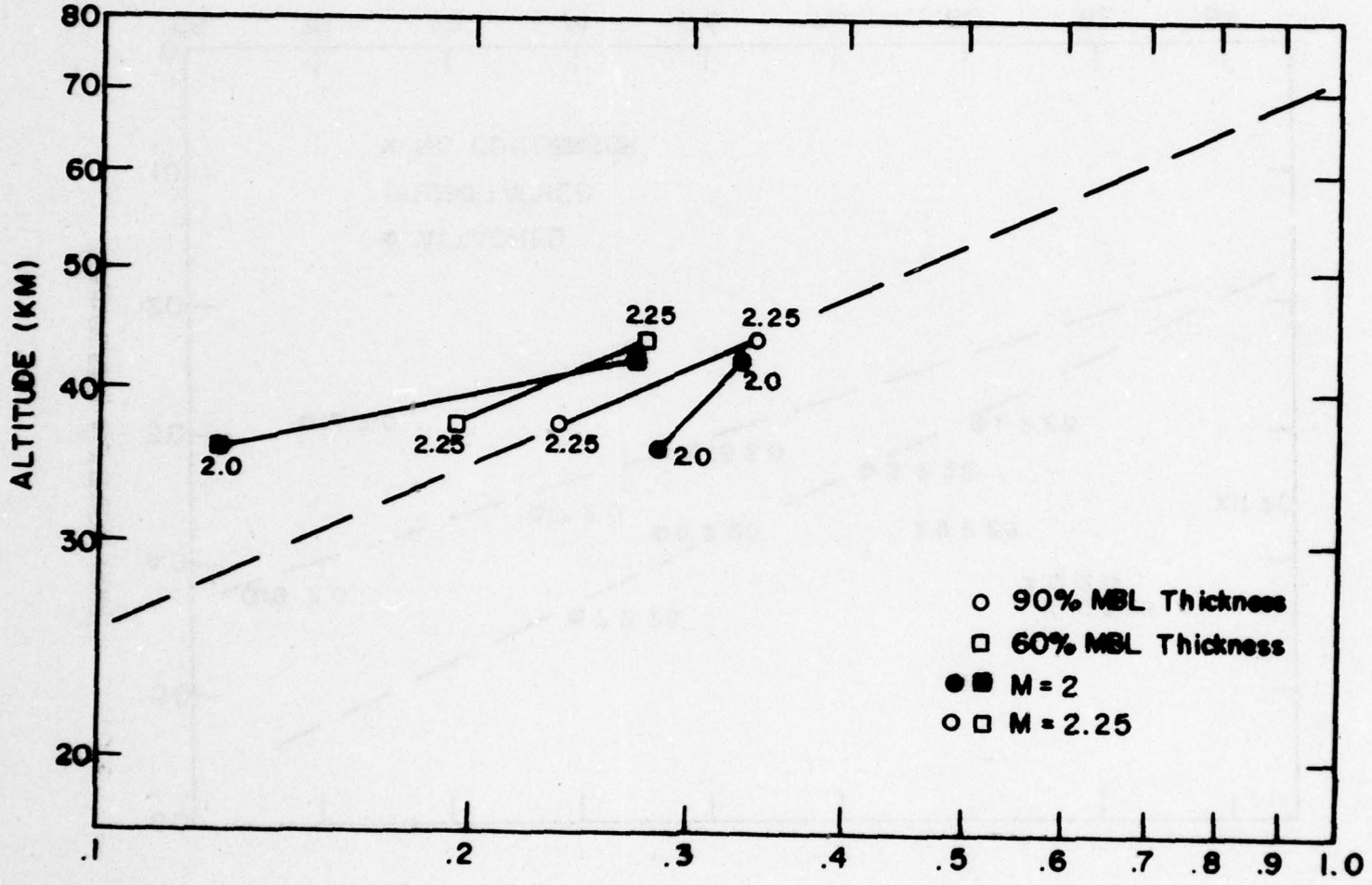

Figure 13. BL THICKNESS INCHES ON 1/4 SCALE MODEL

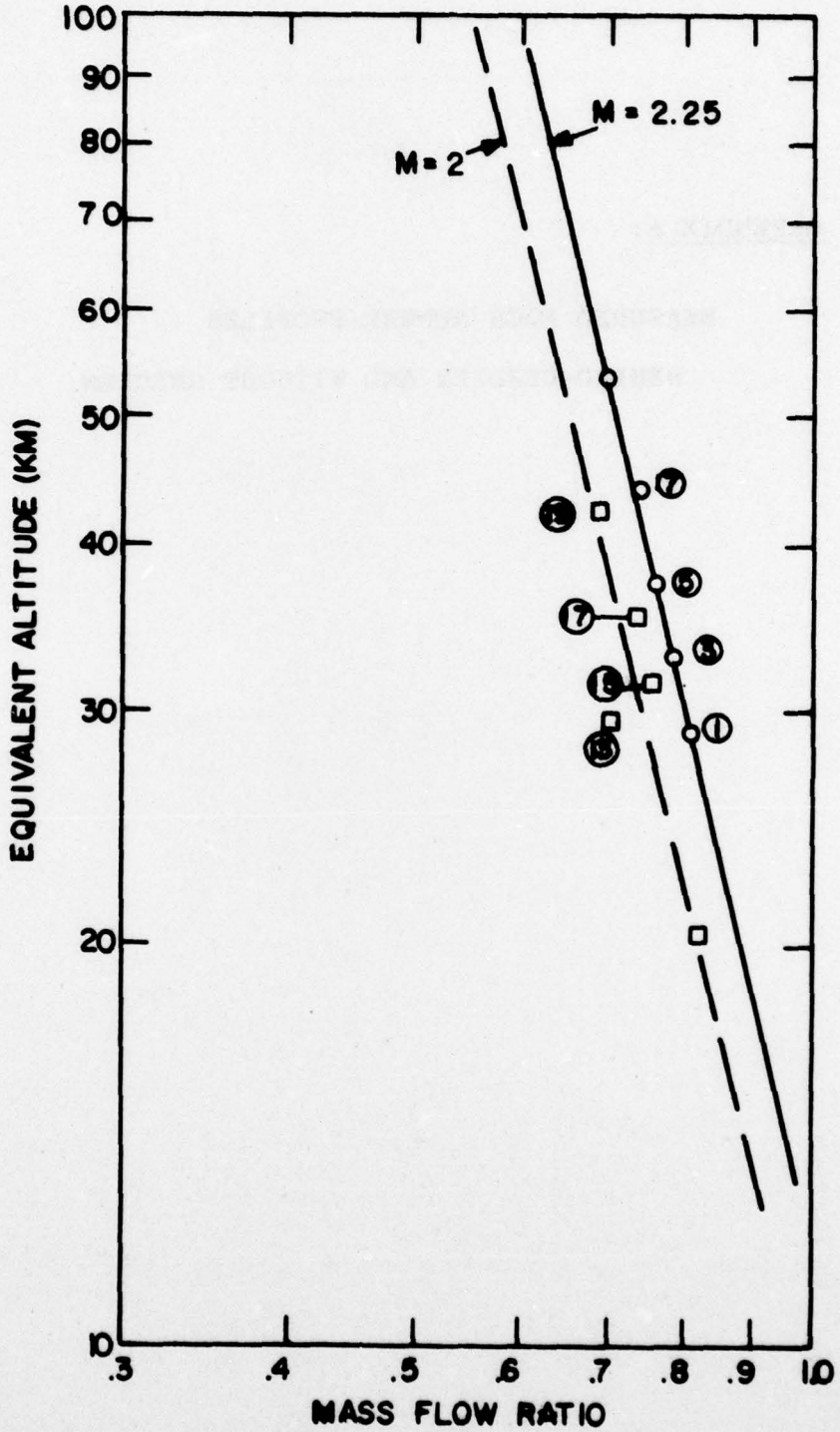

Figure 14. Log log plot of mass flow ratio vs. altitude.

APPENDIX A:

MEASURED MACH NUMBER PROFILES

BEHIND GERDIEN AND WITHOUT GERDIEN

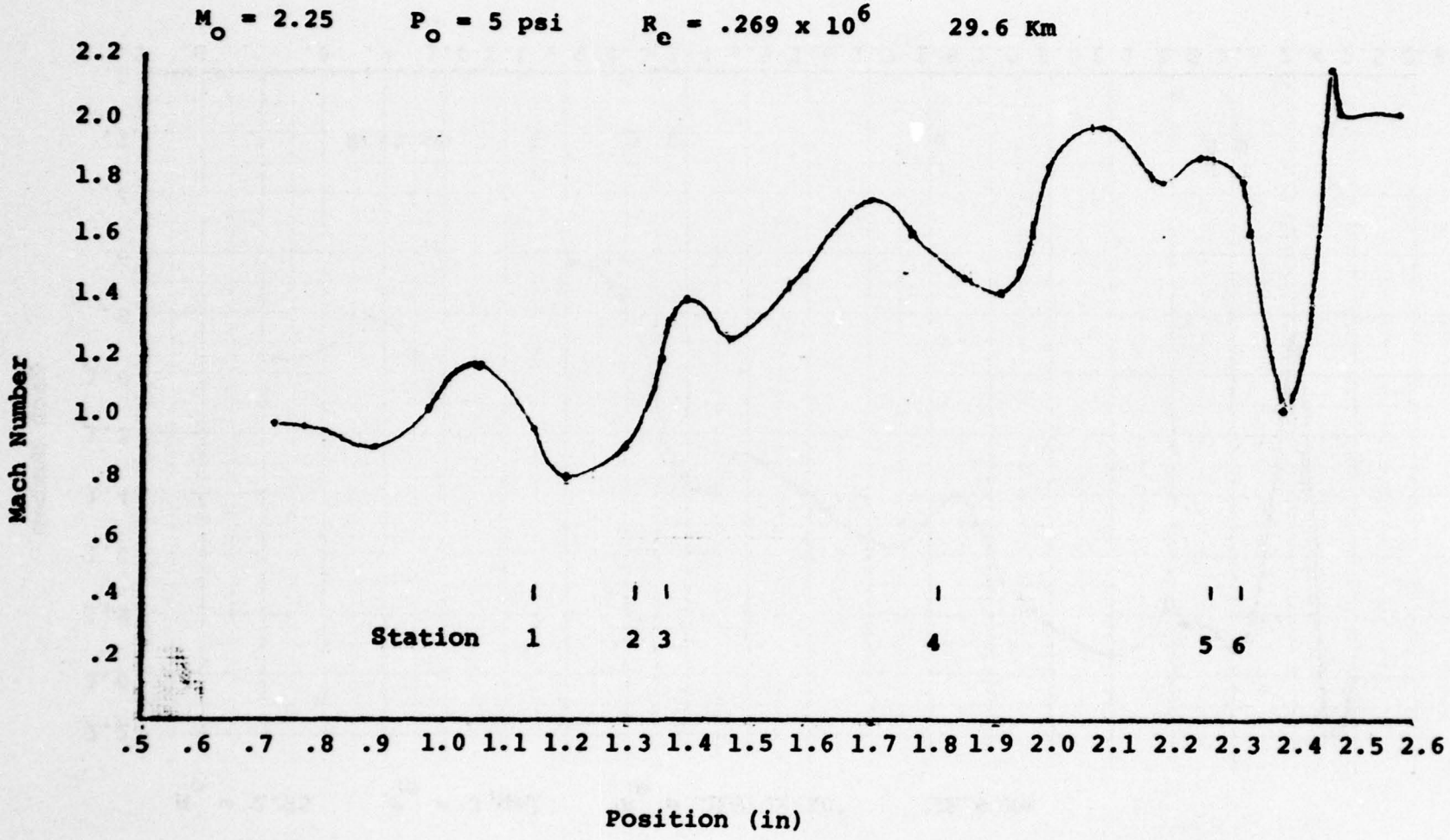

Figure A-1. Mach Number Profile behind Gerdien Capacitor for Run 1

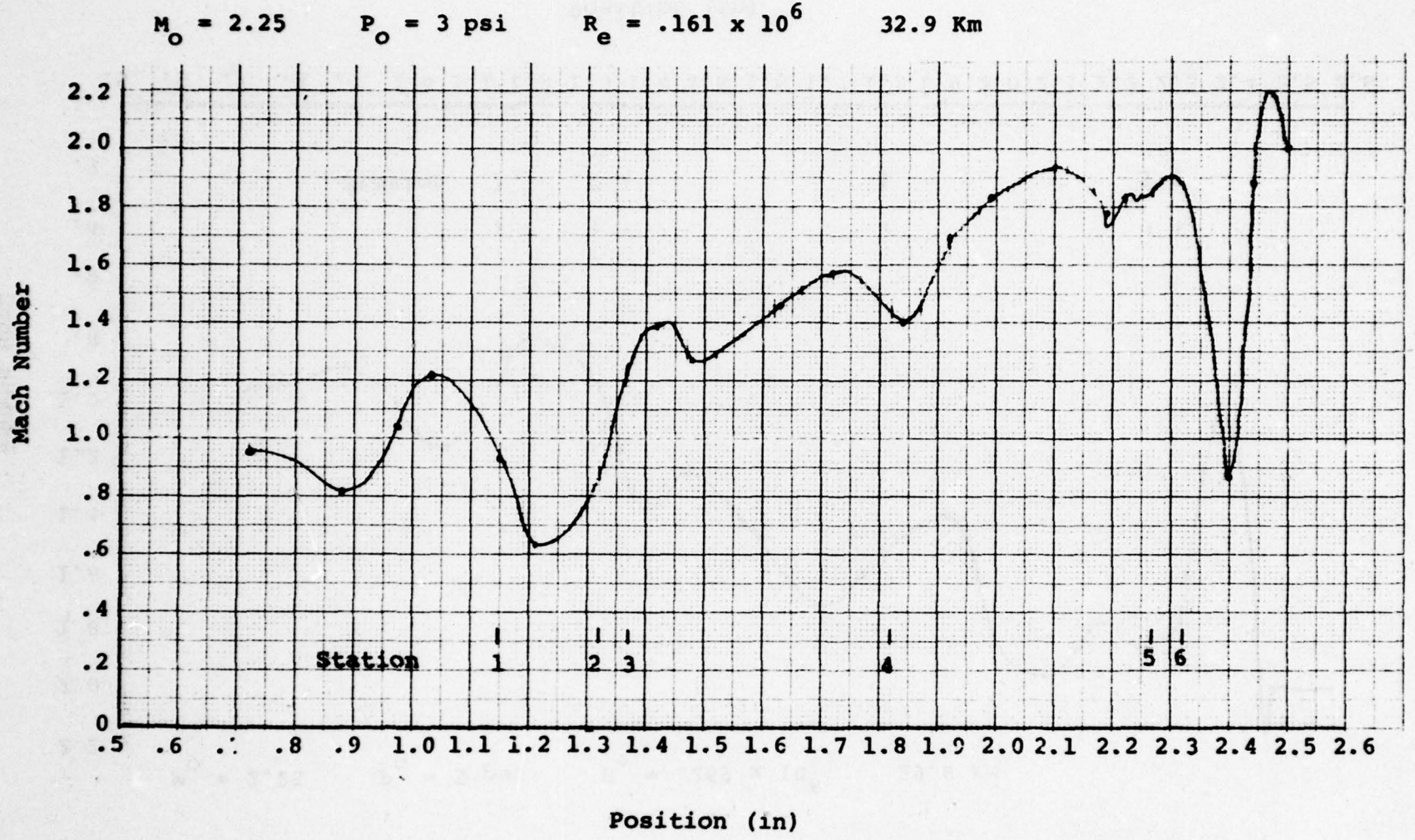

Figure A-2. Mach Number Profile behind Gerdien Capacitor for Run 3

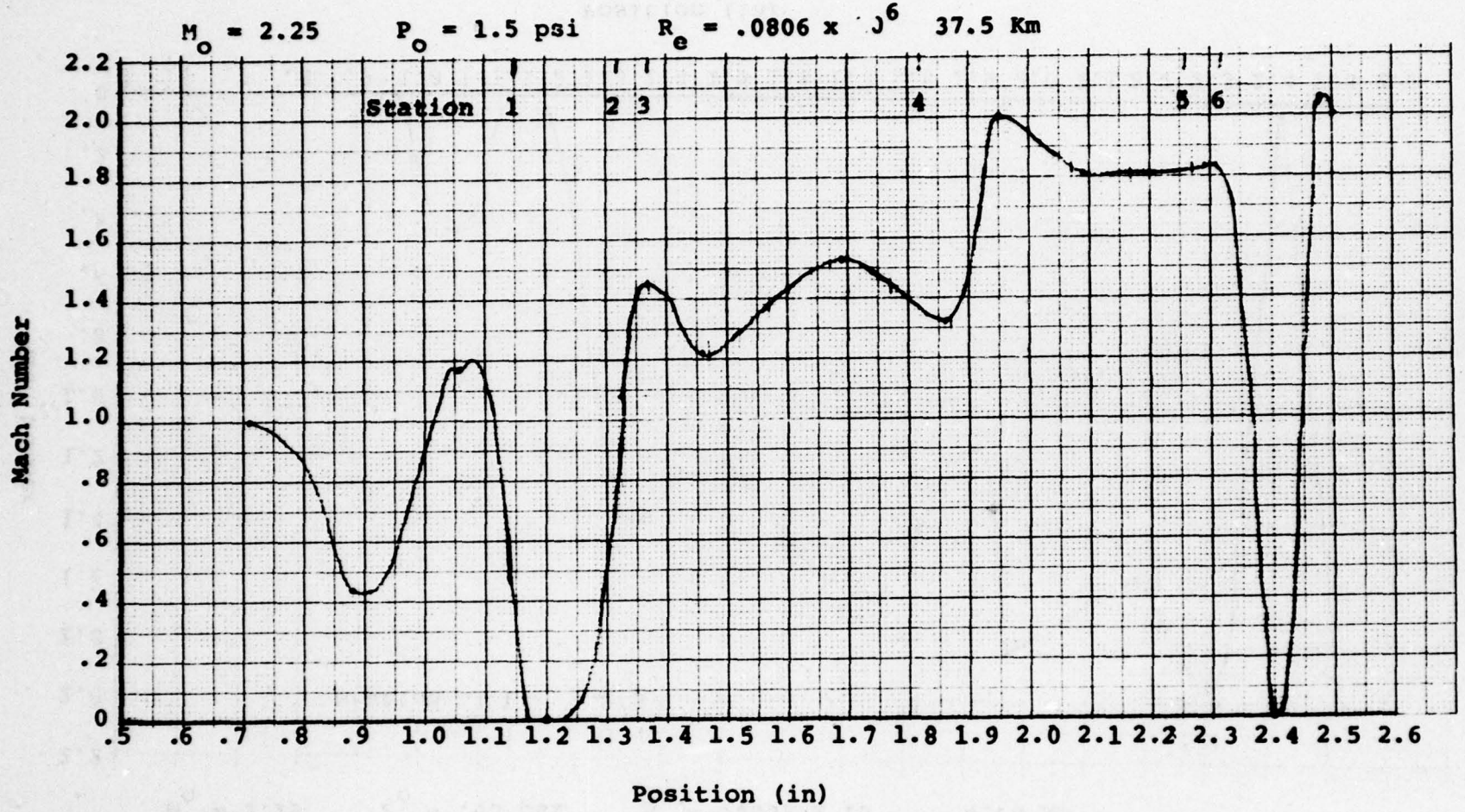

Figure A-3. Mach Number Profile behind Gerdien Capacitor for Run 5

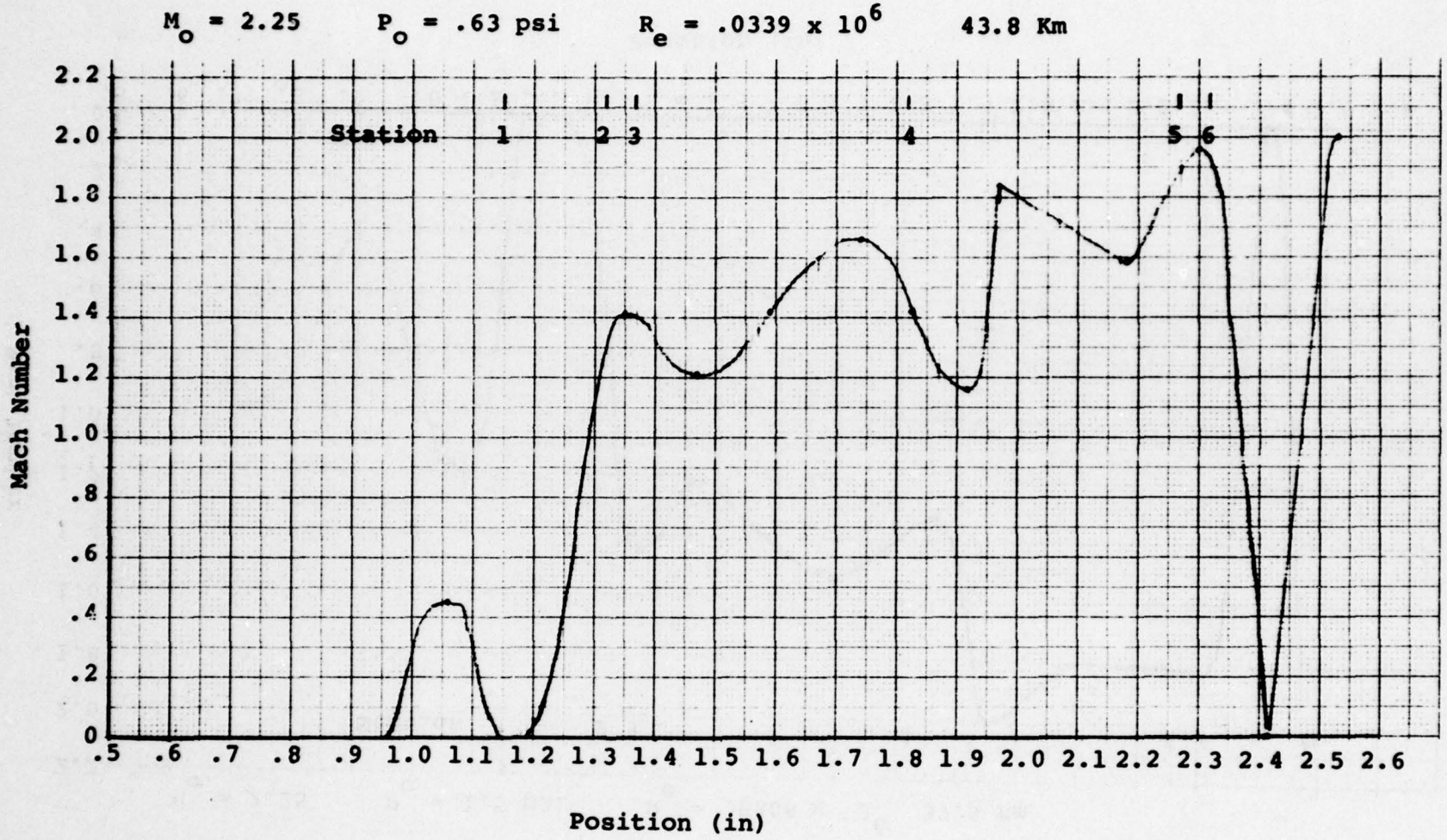

Figure A-4. Mach Number Profile behind Gerdien Capacitor for Run 7

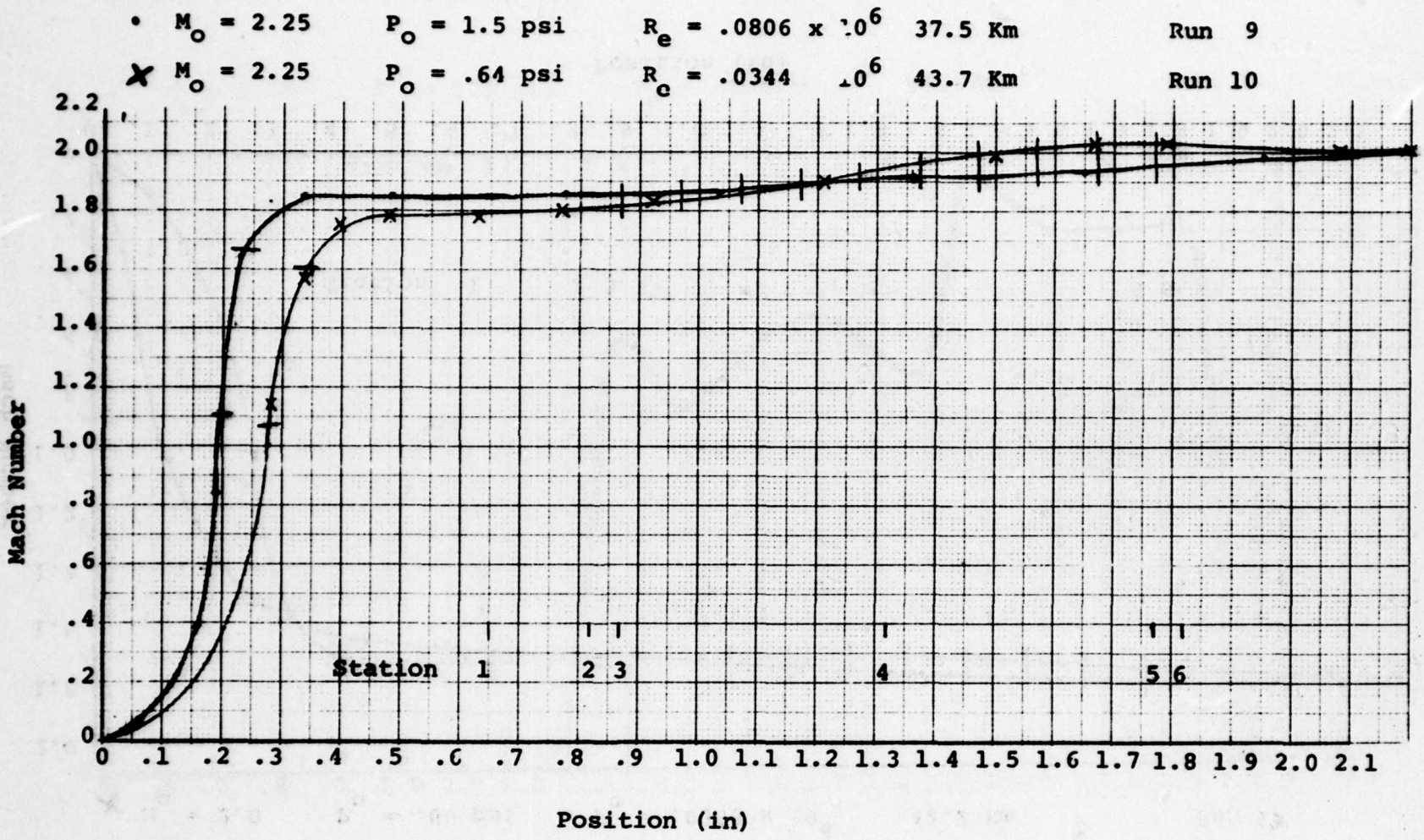

Figure A-5. Mach Number Profile without Gerdien for Runs 9 and 10

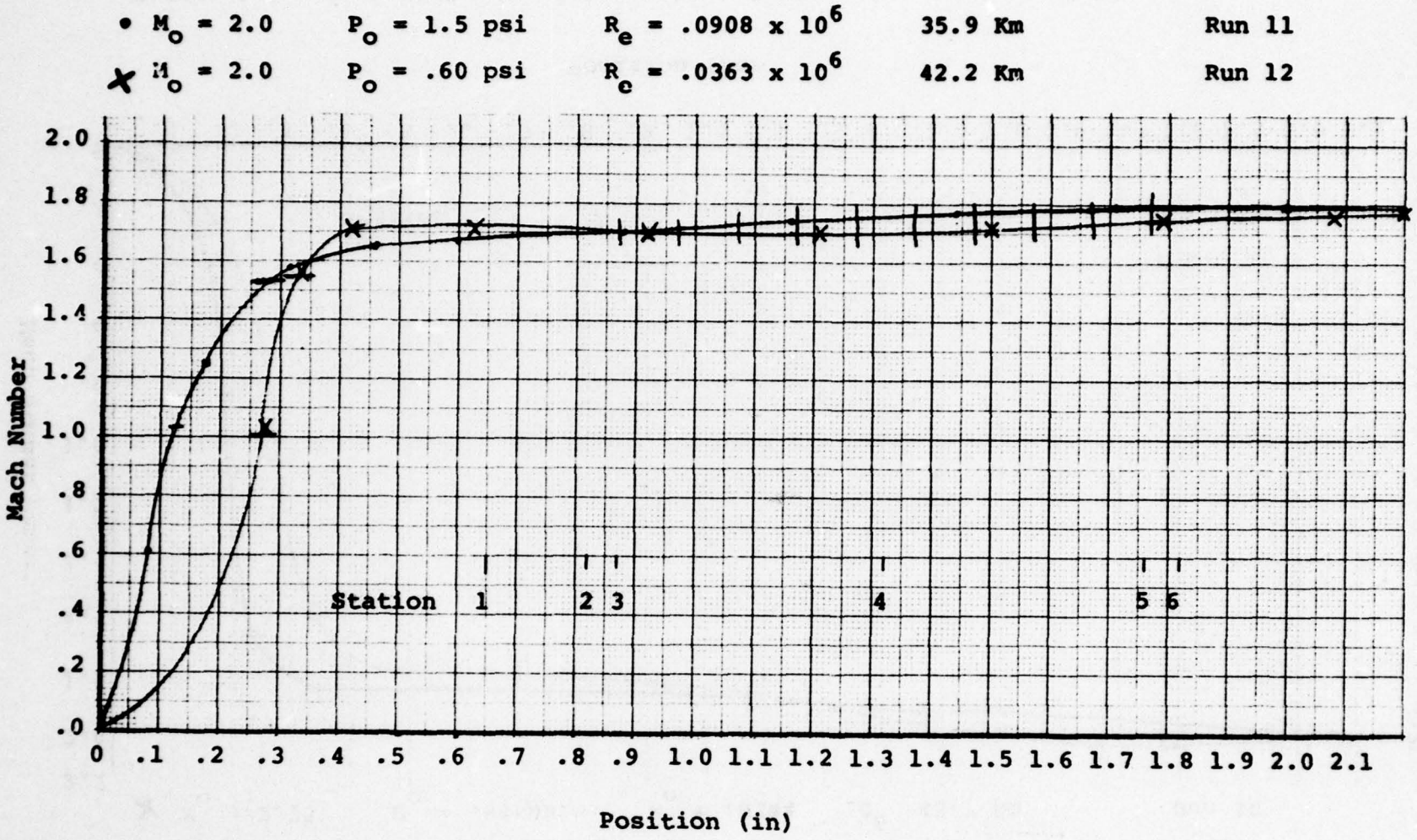

Figure A-6. Mach Number Profile without Gerdien for Runs 11 and 12

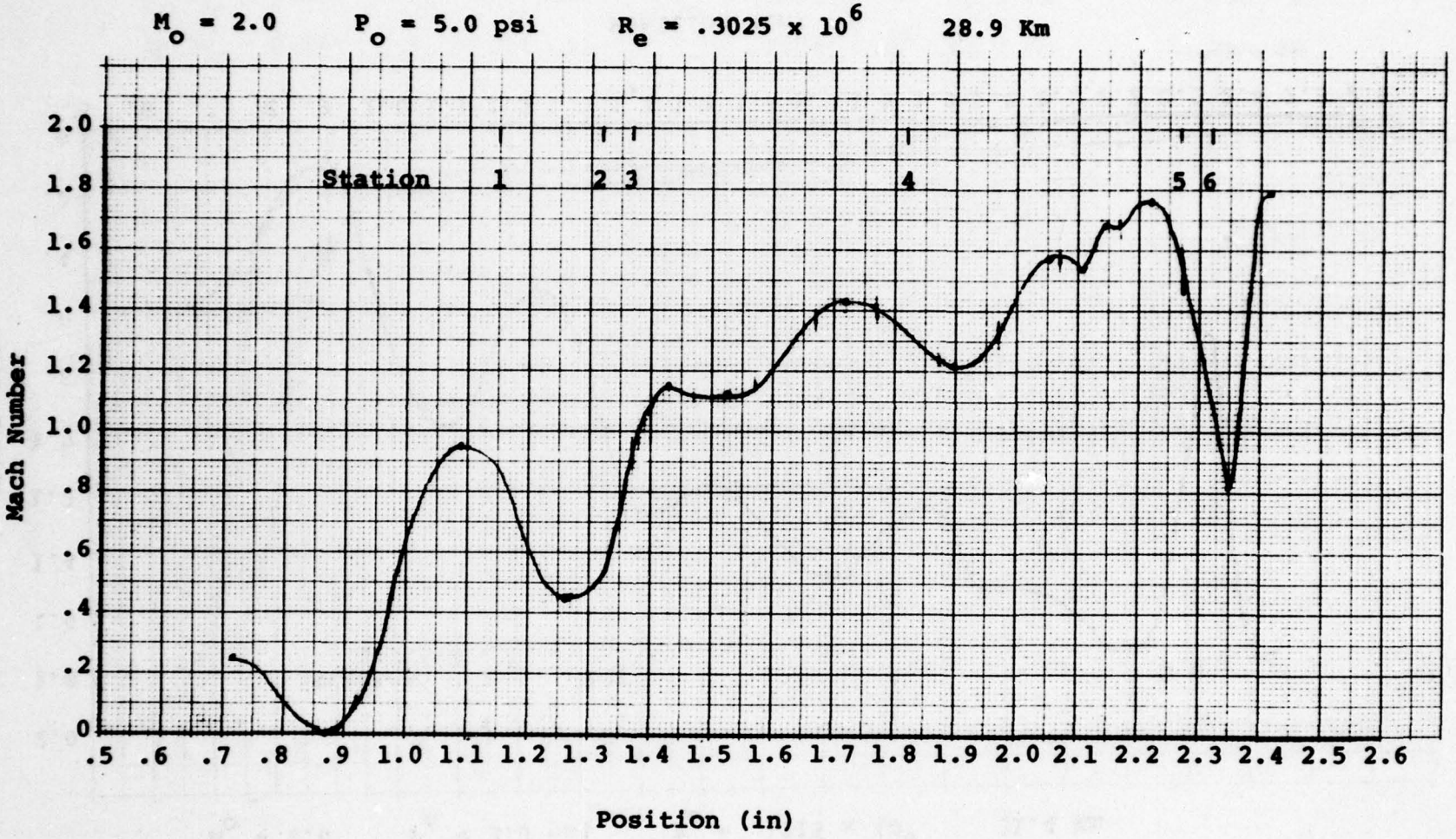

Figure A-7. Mach Number Profile behind Gerdien Capacitor for Run 13

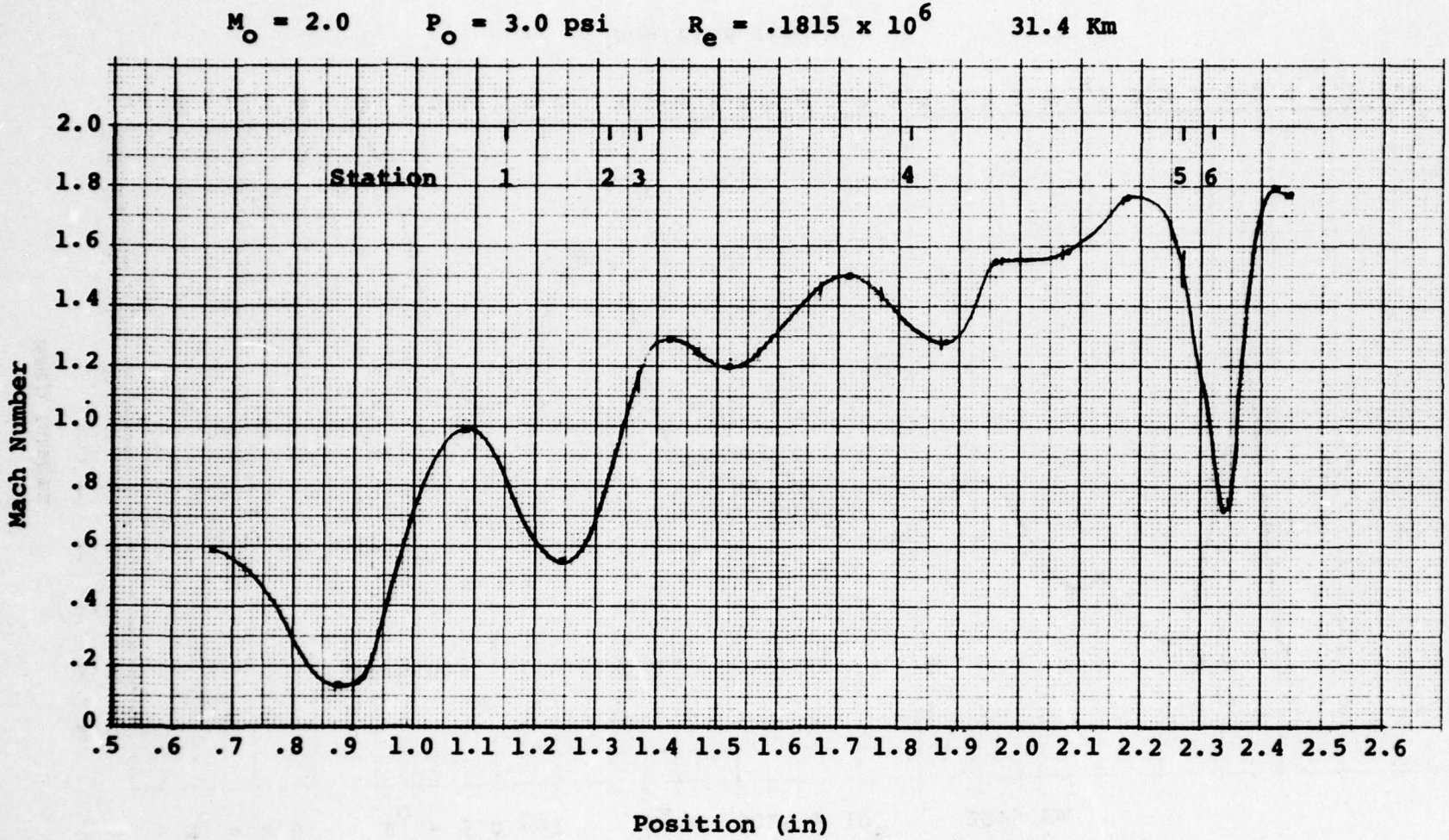

Figure A-8. Mach Number Profile behind Gerdien Capacitor for Run 15

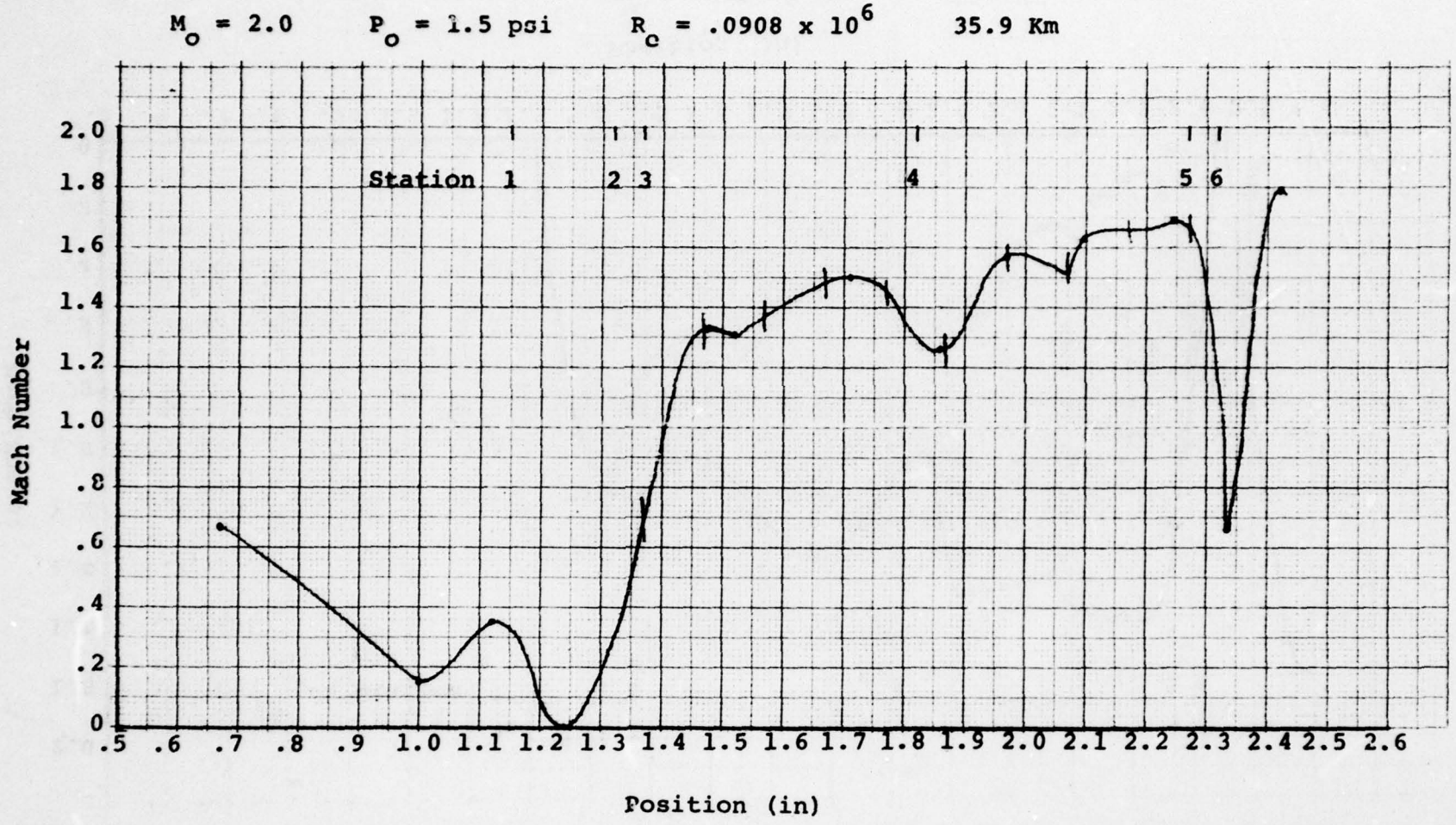

Figure A-9. Mach Number Profile behind Gerdien Capacitor for Run 17

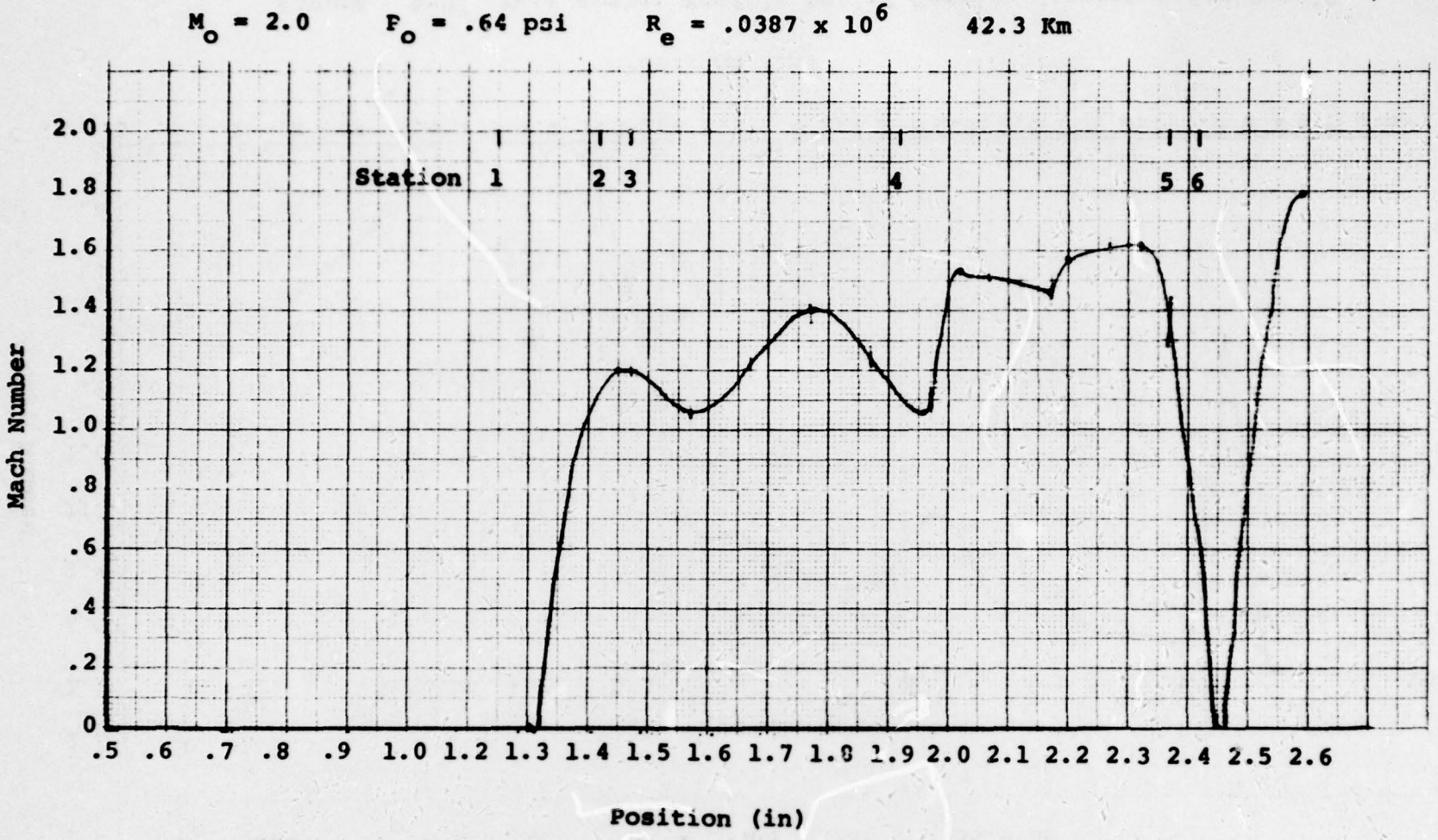

Figure A-10. Mach Number Profile behind Gerdien Capacitor for Run 14